Australian Journal of Earth Sciences (2000) **47**, 179–208

Evaporites, brines and base metals: low-temperature ore emplacement controlled by evaporite diagenesis

J. K. WARREN*

JK Resources Pty Ltd, PO Box 520, Mitcham, SA 5062, Australia.

Salt beds and salt allochthons are transient features in most sedimentary basins, which through their dissolution can carry, focus and fix base metals. The mineralisation can be subsalt, intrasalt or suprasalt, and the salt body or its breccia can be bedded or halokinetic. In all these evaporite-associated low-temperature diagenetic ore deposits there are four common factors that can be used to recognise suitably prepared ground for mineralisation: (i) a dissolving evaporite bed acts either as a supplier of chloride-rich basinal brines capable of leaching metals, or as a supplier of sulfur and organics that can fix metals; (ii) where the dissolving bed is acting as a supplier of chloride-rich brines, there is a suitable nearby source of metals that can be leached by these basinal brines (redbeds, thick shales, volcaniclastics, basalts); (iii) there is a stable redox interface where these metalliferous chloride-rich waters mix with anoxic waters within a pore-fluid environment that is rich in organics and sulfate/sulfide/H_2S; and (iv) there is a salt-induced focusing mechanism that allows for a stable, long-term maintenance of the redox front, e.g. the underbelly of the salt bed or allochthon (subsalt deposits), dissolution or halokinetically maintained fault activity in the overburden (suprasalt deposits), or a stratabound intrabed evaporite dissolution front (intrasalt deposits). The diagenetic evaporite – base-metal association includes world-class Cu deposits, such as the Kupferschiefer-style Lubin deposits of Poland and the large accumulations in the Dzhezkazgan region of Kazakhstan. The Lubin deposits are subsalt and occur where long-term dissolution of salt, in conjunction with upwelling metalliferous basin brines, created a stable redox front, now indicated by the facies of the Rote Faule. The Dzhezkazgan deposits (as well as smaller scale Lisbon Valley style deposits) are suprasalt halokinetic features and formed where a dissolving halite-dominated salt dome maintained a structural focus to a regional redox interface. Halokinesis and dissolution of the salt bed also drove the subsalt circulation system whereby metalliferous saline brines convectively leached underlying sediments. In both scenarios, the resulting redox-precipitated sulfides are zoned and arranged in the order Cu, Pb, Zn as one moves away from the zone of salt-solution supplied brines. This redox zonation can be used as a regional pointer to both mineralisation and, more academically, to the position of a former salt bed. In the fault-fed suprasalt accumulations the feeder faults were typically created and maintained by the jiggling of brittle overburden blocks atop a moving and dissolving salt unit. A similar mechanism localises many of the caprock replacement haloes seen in the diapiric provinces of the Gulf of Mexico and Northern Africa. Evaporite-associated Pb–Zn deposits, like Cu deposits, are focused by brine flows associated with both bedded and halokinetic salt units or their residues. Stratabound deposits, such as Gays River and Cadjebut, have formed immediately adjacent to or within the bedded salt body, with the bedded sulfate acting as a sulfur source. In allochthon/diapir deposits the Pb–Zn mineralisation can occur both within a caprock or adjacent to the salt structure as replacements of peridiapiric organic-rich pyritic sediments. In the latter case the conditions of bottom anoxia that allowed the preservation of pyrite were created by the presence of brine springs and seeps fed from the dissolution of nearby salt sheets and diapirs. The deposits in the peridiapiric group tend to be widespread, but individual deposits tend to be relatively small and many are subeconomic. However, their occurrence indicates an active metal-cycling mechanism in the basin. Given the right association of salt allochthon, tectonics, source substrate and brine ponding, the system can form much less common but world-class deposits where base-metal sulfides replaced pyritic laminites at burial depths ranging from centimetres to kilometres. This set of diagenetic brine-focusing mechanisms are active today beneath the floor of the Atlantis II Deep and are thought to have their ancient counterparts in some Proterozoic sedex deposits. The position of the allochthon, its lateral continuity, and the type of sediment it overlies controls the size of the accumulation and whether it is Cu or Pb–Zn dominated.

KEY WORDS: base metals, copper, diagenesis, evaporites, lead, mineral deposits, salt tectonics, zinc.

INTRODUCTION

In this the third and final review on the metal–evaporite association (Warren 1996, 1997) I hope to show that most subsurface evaporites ultimately dissolve and, through their ongoing dissolution and alteration, create conditions suitable for metal enrichment and entrapment. In most sedimentary/metasedimentary fluid-flow systems, a mineralisation event is part of an ongoing burial history that is preserved in the textures of the rock matrix. One should see the role of evaporites and metal sulfides as each

*Present address: Department Petroleum Geosciences, University Brunei Darussalam, Tungku Link, Bandar Seri Begawan, Brunei (jwarren@brunet.bn).

contributing its part to this larger scale 'mineral systems' approach. Ore deposits are no more than part of the ongoing fluid evolution and burial story. Ore paragenesis should be integrated with a framework of regional geology, sedimentology, diagenetic–metamorphic–igneous facies, fluid-flow conduits and structural evolution. In this way, a predictive model can be garnered from a detailed analysis of the rock matrix.

For clarity, this review is divided into three parts: first, a discussion of evaporite-related fluids that carry and focus the precipitation of metals; second, those ore deposits where the evaporite presence is unequivocal, either through the remaining presence of evaporite salts, or the presence of more than one indicator of former evaporites; and third, a discussion of salt allochthon/laminite deposits where the evidence for the association is more enigmatic.

EVAPORITES AND FLUIDS IN THE SUBSURFACE

Before, or as, subsurface evaporites dissolve, they can transport, seal, trap, focus and precipitate ore from basinal fluids. Thus a subsurface evaporite unit acts as:

(1) Brine and ion source. As the salt dissolves it acts as a brine or volatile source feeding high salinity brines into the basin hydrology. It can supply economically important ions that, depending on the dissolving mineralogy, may be either metalliferous and chloride-rich or metal-poor sources of sulfur.

(2) Seal and trap. Thick evaporite units act as a seal to the free escape of basinal, hydrothermal, hybrid or upwelling meteoric waters. Given the right geometry, an evaporite unit can also act as a fluid trap that, until it is breached, will pond beneath it any escaping metalliferous basinal waters and hydrocarbons.

(3) Focus. Breach points or zones in the evaporite bed created by flowage (halokinesis), décollement, or faulting tend to focus the escape of pressured basinal waters into the zones above or sometimes even below the breach. Hot metalliferous basinal water escaping into near-surface and surface settings can then create sea-floor brine lakes and replacement haloes about, or near, the trap position or along the escape conduit.

That is, in the case of a thick basin-wide evaporite succession, a dissolving evaporite bed or allochthon in its more deeply buried halite-rich basin centre position may be supplying metal-leaching chloride brine to suprasalt and subsalt convective plumes. At the same time, at positions higher in the stratigraphy or further out toward more shallowly buried basin margin, the same salt can focus this metal-carrying brine into outflow zones where the metals are fixed by the reduction of sulfate–evaporite beds. Even after the salts in a basin have gone, the zone of dissolution residues can continue to act as an aquifer or focus for ongoing metalliferous brine flow. Recognising the process and timing under which an evaporite disappeared is often the most important step in understanding the evaporite/base-metal association. This is especially true of Proterozoic and Archaean base-metal deposits where no actual salts remain, only indicators of former evaporites.

Ore-fluid chemistry ('metal carriers')

The chemical make-up of any brine created by evaporite dissolution depends on the mineralogy of the dissolving sequence. Thick beds of halite (the most common basin-wide evaporite) generate chloride-rich brines that are capable of carrying metals; while leached anhydrite/gypsum successions are likely to develop more sulfate- or sulfide-enriched waters (depending on the oxidation state at the site of dissolution). Most high chlorinity subsurface waters are not connate (i.e. not preserved seawater), but are generated through pore-water – salt bed interaction during burial. For example, chloride-dominated deep brines in the Canning Basin and beneath the modern Gulf of Mexico are the result of dissolution of thick buried halite beds (Ferguson *et al.* 1992, 1993; Land 1995a, b).

In order to qualify as a potential ore-carrying fluid, a basinal fluid must contain on the order of 1 mg/L or more of the dissolved metal in question (Figure 1a) (Eugster 1989; Hanor 1994). Most basinal brines that achieve Pb, Zn or Cu values at or above this level have pore salinities that are typically in excess of 200 000 mg/L, with their entrained base metals carried as chloride complexes. These waters also have high chloride concentrations, lowered pH, and most occur in basins that contain, or once contained, thick dissolving salt beds. The capacity of chloride-rich basinal brines to become ore-forming fluids is well illustrated by the Na–Ca–Cl oilfield brines in the Cheleken region of Turkmenistan (Lebedev 1972). These brines contain up to 10 mg/L Zn+Pb and deposit native lead, sphalerite, galena and pyrite in the well pipes and holding tanks at rates

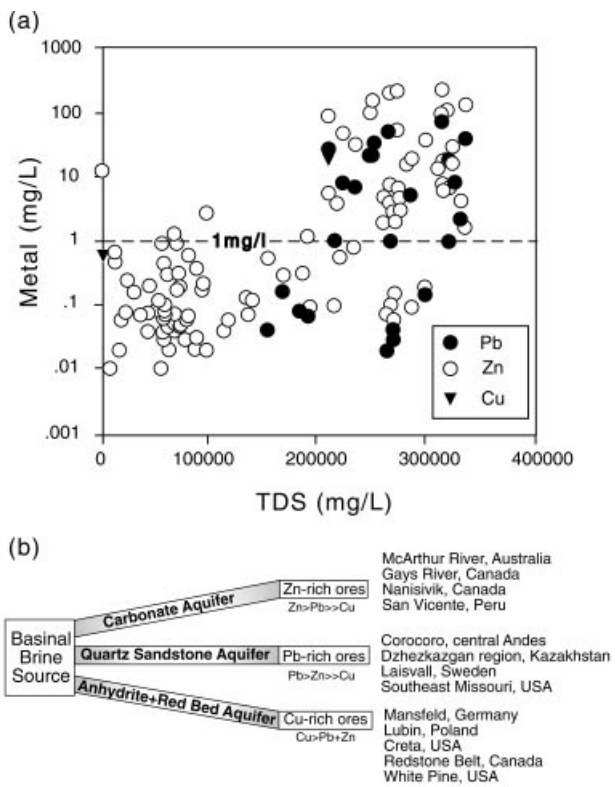

Figure 1 (a) Metal content of selected subsurface waters worldwide (after Hanor 1994). (b) Effect on metal content of aquifer lithology and examples of the resulting ore deposits (after Sverjensky 1989).

analogous to ore formation. Some Na–Ca–Cl oilfield brines in Jurassic and Cretaceous formations in the Salt Dome Basin of central Mississippi, USA, have total dissolved solid contents up to 350 000 mg/L , densities that exceed 1.2 g/mL, and contain up to several hundred mg/L of Pb + Zn (Carpenter *et al*. 1974; Kharaka *et al*. 1987). Both these highly metalliferous brines occur in regions underlain by thick dissolving evaporite sequences.

Sphalerite and galena scale is forming today in the pipes of producing geothermal wells in the Asal Rift in the Republic of Djibouti, Africa (Damore *et al*. 1998). Sulfide precipitation starts at the flash level of these chloride-rich brines, located at 850 m depth where temperatures are close to 260°C, and extends deeper into the main geothermal reservoir. The main reservoir is located at depths between 1000 and 1300 m with temperatures between 260 and 360°C. Seawater seepage, with input from dissolving salt beds, is the main brine source in the field. As a result of sulfide precipitation, about 90% of H_2S is removed from the original fluid before it is discharged at the surface. Brines produced in the Asal thermal field all have salinities in excess of 100 000 ppm, with a low gas content of the order of 0.6 mmol/mol.

Much of the metal content in these brines has an intrabasinal non-magmatic source. Some researchers proposed that the metals in basinal brines are derived either from the alteration and leaching of feldspars and clays to supply most of the iron, lead, barium and strontium, or from the alteration of carbonates to supply most of the zinc (Land & Prezbindowski 1981; Sverjensky 1986; Kharaka *et al*. 1987). Sverjensky (1989) further refined earlier brine-transport models by demonstrating that significant water–rock interaction takes place as warm, basinal chloride-rich brines traverse and interact with various aquifers. He concluded that, depending on the dominant lithology of the aquifer traversed by the brines, a single basinal brine may evolve chemically to become the ore-forming fluid for a wide range of sediment-hosted base-metal sulfide deposits. Migration through carbonate, quartz sandstone, or anhydrite + redbed aquifers could result in the formation of Zn-, Pb-, or Cu-rich deposits, respectively (Figure 1b). As a starting point he considered a typical chloride-enriched basinal brine that was initially saturated with galena, chalcopyrite, muscovite, kaolinite and quartz, but undersaturated with respect to sphalerite, with up to 1 mg/L Pb, 0.1 mg/L Cu and 5 mg/L Zn. Passage of this fluid through a carbonate-cemented aquifer produces a metalliferous brine characterised by high Zn/Pb and (Zn + Pb)/Cu ratios. Transport of the same fluids through a quartz-cemented sandstone exhausts the buffering capacity of the aquifer relatively quickly, so that any mineral accumulations precipitated from the resulting waters are galena-rich. Maintenance of the oxidation state in a typical basinal brine near the hematite–magnetite buffer prevents copper mobilisation (solubility of Cu in a typical basinal brine is ≈ 0.07 mg/L). However, if the basinal brine migrates though a redbed succession that contains hematite and/or anhydrite, the oxidation state and the SO_4^{2-}/H_2S ratio of the fluid are increased by reactions such as:

$$CaSO_4 = Ca^{2+} + SO_4^{2-}$$

$$4Fe_2O_3 + H_2S + 14\ H^+ = 8\ Fe^{2+} + SO_4^{2-} + 8H_2O$$

The migration of this more oxidising fluid through a redbed can then scavenge the necessary Cu, Zn and Pb to form a mineralising fluid with elevated Cu content (Cu > Pb + Zn). Redox conditions of $\log f_{O_2} > -46$ at 125°C are necessary in the brine to mobilise copper as cuprous chloride complexes. This explains the common association of copper sulfides with reduction haloes adjacent to redbeds (see later).

Figure 1a clearly shows that many highly saline basinal waters in sedimentary basins worldwide contain <1 ppm metal. Acidification is an essential step in the acquisition of metals during dissolution of aquifer minerals. Chloride-rich, high-salinity basinal fluids may become acidified by pyrite oxidation, by decomposition of organic matter, or by the precipitation of Mg silicates, such as smectite or chlorite. Organic acids may also play an important role in leaching the metals from metalliferous source beds (Raiswell & Al-Biatty 1992). In contrast, Eugster (1985, 1989) argued that not all metalliferous brines are acidic. In a Green River style of ore deposit (in which Eugster includes the Mt Isa and Dugald River deposits of Australia) the brines were alkaline with pH values of up to 11. Metals were carried not as chloride-complexes, but as hydroxy- or carbonate-complexes. Such non-chloride waters are generated today in saline continental rift lakes where sodium bicarbonate evaporites dominate, there is no primary gypsum, and the lake evolves by the evaporation of source waters that drain adjacent basic igneous or metamorphic terranes.

Sulfur redox reactions

Redox fronts are mostly subsurface interfaces where base metals can precipitate. Such fronts are typically created by the presence of H_2S and organic matter on the reducing anoxic side of the interface and metalliferous chloride-rich waters on the other side (Figure 2a). Much of the H_2S in a sedimentary basin is produced in reducing conditions generated by sulfate reduction, although it can also be generated from magmatic sources. In the resulting base-metal deposits the fixing of the copper, lead and zinc was a low-temperature diagenetic reaction between abundant reduced sulfur in the host (from sulfate reduction, pyrite, H_2S) and base metals carried into these deposits via saline chloride-rich brines. The zone of reduced sediment is an excellent chemical trap for the metals and is often defined by a colour change from red (oxidised iron) to grey-green (reduced iron). The reduction process can be bacterially mediated through the activities of sulfate-reducing bacteria (bacterial sulfate reduction—BSR) or inorganically mediated under conditions of increased temperature and pressure (thermochemical sulfate reduction—TSR). Both scenarios require the presence of preserved organic matter or its more evolved subsurface equivalent in the form of hydrocarbons (oil or gas).

BACTERIAL SULFATE REDUCTION

During bacterial sulfate reduction, bacteria produce H_2S at temperatures less than 80–110°C (Figure 2b) (Trudinger *et al*. 1985; Hill 1995; Riciputi *et al*. 1996; Aref 1998). For example, the strictly anaerobic, sulfur-reducing bacteria (*Desulfo*-x) produces isotopically light H_2S by metabolising

organic matter (or hydrocarbons) with sulfate as the oxidising agent:

$$Ca^{2+} + 2SO_4^{2-} + 2CH_4 + 2H^+ \rightarrow 2\,H_2S + CaCO_3 + 3H_2O + CO_2$$

In this equation, CH_4 represents a host of possible organic compounds or hydrocarbons and SO_4 is dissolved sulfate either from shallow phreatic refluxing brines or from dissolved sulfate evaporites such as gypsum, glauberite or anhydrite. $CaCO_3$ represents bioepigenetic limestone products that often precipitate as replacements of precursor evaporite sulfates (e.g. calcitic caprocks of the Gulf Coast diapirs and the Castile mounds of west Texas).

Bacterial sulfate reduction in and beneath dense anoxic brines and shallow subsurface brines explains the abundance of early pyrite in the sediments of many density-stratified brine lakes and seaways and its preponderance in many Archaean oceanic sediments. In the presence of soluble ferrous iron, the sulfide produced during sulfate reduction will immediately precipitate as metastable iron monosulfides, such as mackinawite, greigite and amorphous FeS. These intermediates are kinetically favoured over the direct precipitation of pyrite due to its much lower solubility product. Later they will transform to framboidal pyrite in the shallow subsurface. With time this framboidal form is in turn overgrown by euhedral pyrite. Evidence that early syngenetic biogenic pyrite is subsequently replaced via epigenesis can be seen in many bacterially influenced base-metal laminite deposits, such as Bou Grine in north Africa, McArthur River in Australia and Lubin in Poland (Sawlowicz 1992).

Sulfate-reducing bacteria are ecologically diverse and tend to develop wherever sulfate is present along with a supply of organic matter sufficient to create anaerobic conditions. Their growth is generally restricted to waters with pH values of 5–9. The creation of microniches means there are many additional situations where the bacterial reducers are flourishing locally, while the overall environment exhibits pH levels that are unfavourable to bacterial growth. The upper temperature limit for biogenic sulfate reduction is considered by many to be 80–85°C (Trudinger *et al.* 1985). But under suitably pressurised conditions it may extend into higher temperatures. Recent work in deep-sea hydrothermal vent sediments of the Guaymas Basin in the Gulf of California has revealed archaebacterially mediated sulfate reduction at temperatures up to 110°C, with an optimal rate at 103–106°C (Huber *et al.* 1989; Jørgensen *et al.* 1992).

In the pore fluid of an actively dewatering sedimentary basin, the sulfate-reducing bacteria commonly thrive within, or near, any water–oil contact down to depths of a few kilometres. These are the aerobic/anaerobic (redox) transition zones between reduced paraffinic crude oils and oxygenated groundwaters. Locally anoxic conditions mean the aerobic bacteria provide nutrients to the sulfate-

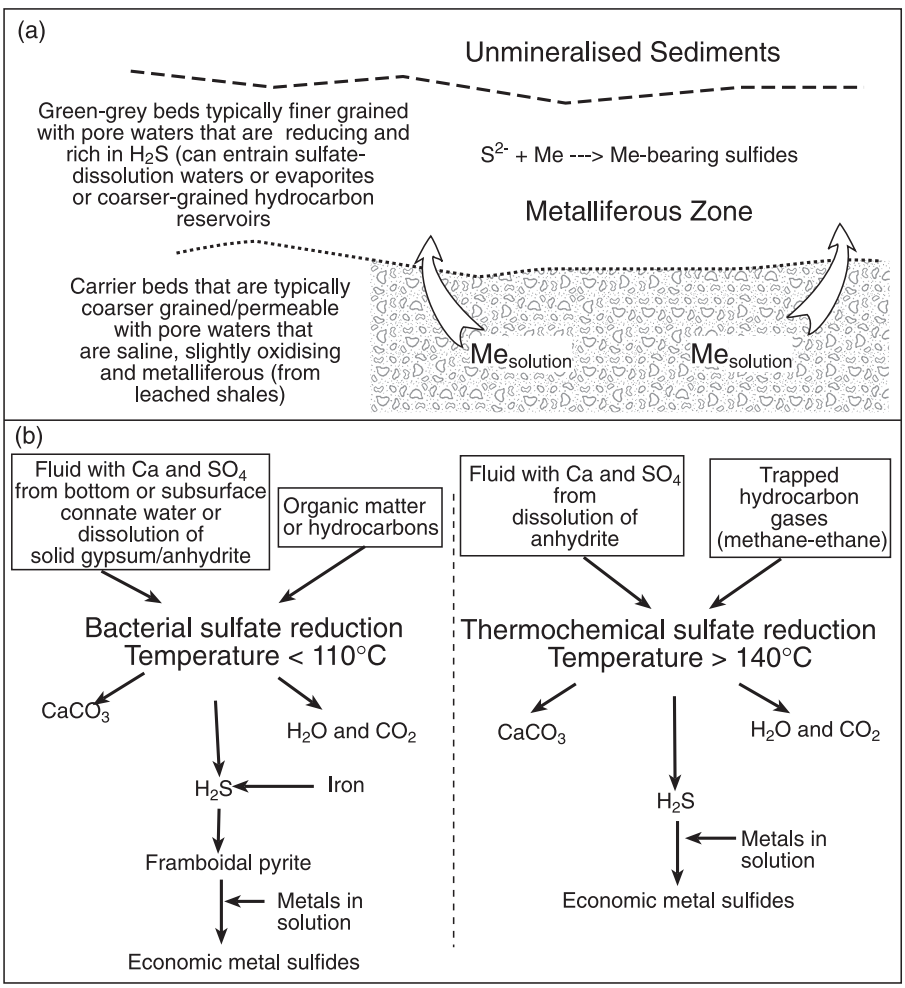

Figure 2 (a) Metal sulfide 'fixing' at redox interfaces (after Brown 1993). (b) Chemical pathways associated with sulfate reduction. Note the lack of biologically produced framboids under thermochemical sulfate reduction (after Warren 1999).

reducing anaerobes. For example, such anoxic interfaces tend to form near the dissolving margins of salt allochthons or diapir caps, where the outflow of reduced basinal waters is focused by the edge of the dissolving salt plumes. The metabolic activities of sulfate-reducing bacteria can also help precipitate metal sulfides at such interfaces (Bechtel *et al*. 1998). Any coprecipitated authigenic carbonates tend to have very negative $\delta^{13}C$ signatures, e.g. the dolomite spar cements found at the gas–water contacts in some Miocene sandstone reservoirs in offshore Brunei have $\delta^{13}C$ values ranging from –20 to –50‰ (JKW unpubl. data). Likewise, the zones of stratabound massive pyrite cements that occur in Triassic reservoir sands in the condensate fields of the North West Shelf, Australia have a similar sulfate reduction genesis (JKW unpubl. data).

Modern sulfate-reducing bacteria also flourish syndepositionally in anoxic water bodies within, or immediately beneath, lacustrine, estuarine, marine and hypersaline environments; there they also contribute to the formation of early pyrite framboids (Demaison & Moore 1980). This geographic isolation of the reducing biota to restricted anoxic bottoms was not so in the Precambrian; under the reducing conditions that typified the Archaean oceans, the whole water column was populated by sulfate-reducing bacteria (Logan *et al*. 1995). Through their metabolism, sulfate-reducing bacteria control the style and amount of organic matter preserved in bottom sediments. The widespread maintenance of an oxygen-stratified oceanic column in the Proterozoic ocean, with a sulfate-reducing bacterial population in the bottom waters of the open ocean and at times on the shelf, played a major role in oceanic circulation patterns and the widespread preservation of pyritic laminites, such as in the organic-rich laminites of the Velkerri Formation in the Roper Group, Northern Territory (Warren *et al*. 1998). Some have even argued that the flowering of the calcareous macrobiota and the marked increase in animal diversity that defines the end of the Proterozoic was brought about by the lowering of the oceanic oxic/anoxic boundary into the sediment column. The lowering was driven by the evolution of organisms that produced faecal pellets. Such pellets rapidly remove organic matter to the ocean bottom, so moving the sulfate-reducing bacteria into these sediments and allowing the encroachment of oxygen to take place throughout the whole water column (Logan *et al*. 1995).

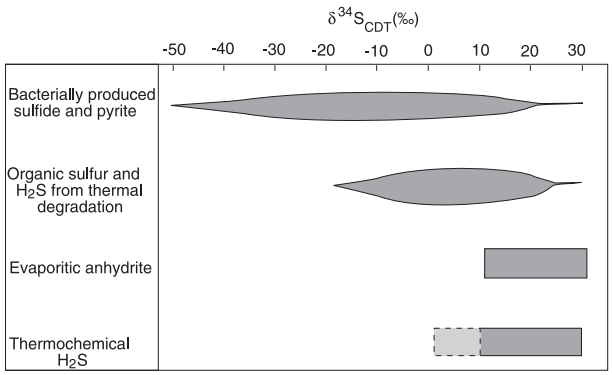

Figure 3 Typical ranges for naturally occurring sulfur isotopes under thermochemical and bacterial sulfate reduction (after Emery & Robinson 1993; Warren 1999).

THERMOCHEMICAL SULFATE REDUCTION

During thermochemical sulfate reduction (TSR), H_2S is produced as sulfate and is inorganically reduced via reactions with hydrocarbons at temperatures in excess of 140°C (Figure 2b) (Heydari 1997). Until recently the efficiency of thermochemical sulfate reduction in producing H_2S was inferred from experimental evidence, or levels of sour gas (H_2S) in oil and gas wells, rather than directly observed in any natural situations (Trudinger *et al*. 1985; Noth 1997). This has now changed with the direct documentation of TSR-produced H_2S (sour gas) in reservoirs in the Permian Khuff Formation of Abu Dhabi (Worden *et al*. 1995, 1996; Worden & Smalley 1996). In reservoirs hotter than 140°C, anhydrite has been partially replaced by calcite, and hydrocarbon gases have been partially or fully replaced by H_2S, that is, anhydrite and hydrocarbons have reacted to produce calcite and H_2S. Carbon and elemental sulfur isotope data from the gases and minerals show that the dominant general reaction is:

$$CaSO_4 + CH_4 \rightarrow CaCO_3 + H_2S + H_2O$$

Gas chemistry and isotope data also show that C_2+ gases reacted preferentially with anhydrite by reactions of the type:

$$2CaSO_4 + C_2H_6 \rightarrow 2CaCO_3 + H_2S + S + 2H_2O$$

Sulfur was generated by this reaction and is locally present, but was also consumed by the reaction:

$$4S + CH_4 + 2H_2O \rightarrow CO_2 + 4H_2S$$

The frequently quoted and experimentally observed reaction between anhydrite and H_2S with CO_2 to produce calcite and sulfur:

$$CaSO_4 + 3H_2S + CO_2 \rightarrow CaCO_3 + 4S + 3H_2O$$

has been shown, by gas chemistry, calcite $\delta^{13}C$ and sulfur $\delta^{34}S$ data, to be insignificant in the Khuff Formation. Rather, the direct reaction between hydrocarbons and anhydrite occurs in solution. It takes place within residual pore waters that are initially dominated by carbonate dissolved from the marine carbonate matrix. The first-formed replacive calcite thus contains carbon that was derived principally from a marine dolomite matrix with a $\delta^{13}C$ signature of 0 to +4‰. Continuing reaction leads to the progressive domination of the water by TSR-derived carbonate with a minimum $\delta^{13}C$ of about –31‰.

Thermochemical sulfate reduction also produces substantial volumes of very low salinity subsurface water. The salinity of formation water in evaporite lithologies undergoing thermochemical sulfate reduction is, therefore, not necessarily high. In the Khuff reservoir the water salinity and isotope data show that the original formation water was diluted between four and five times by water from thermochemical sulfate reduction (Worden *et al*. 1996). A typical Khuff gas reservoir rock volume suggests that initial formation water volumes can only be increased by about three times as a result of thermochemical sulfate reduction. The extreme local dilution shown by the water salinity and $\delta^{18}O$ data in the Khuff must, therefore, reflect transiently imperfect mixing between TSR water and original formation water. Dissipation of this water into surrounding rocks may aid further dissolution of adjacent evaporites.

Sulfate reduction and metallogeny

H_2S (sour gas) is a major product of both bacterial sulfate reduction and thermochemical sulfate reduction (Figure 2b). Wherever it encounters a metalliferous brine this H_2S can then be involved in a number of metal sulfide forming reactions that often also involve alteration/dissolution of the adjacent rock matrix. Sulfide products range from the cool shallow precipitation of syngenetic framboidal pyrite to the formation of hot, hydrothermal sulfides. For example, under a Mississippi Valley type scenario, a metal sulfide phase typically coprecipitates with hydrothermal or saddle dolomite at temperatures in the range of 60–180°C (Hill 1995):

$$H_2S + CO_2 + MeCl^+ + Mg^{2+} + 2CaCO_3 + H_2O \rightarrow$$

$$MeS + Ca^{2+} + CaMg(CO_3)_2 + HCO_3^- + Cl^- + 3H^+$$

(where Me could be Cu, Pb or Zn)

When considering the association of sulfate evaporites with mineralisation it is important to realise that it is not the sulfate evaporites that are directly responsible for the precipitation of metal sulfides. Rather, evaporite dissolution or reaction places sulfate/sulfide in a fluid medium so that it can react with hydrocarbons. This sulfate-entraining solution is reduced in the presence of organic matter or hydrocarbons to form H_2S. It is the H_2S in solution that then precipitates the metal sulfides at or near a redox interface, a zone where slightly more oxidised metalliferous chloride brines can interact with a H_2S buildup on the reduced side of the interface. Thus, the ore textures in areas where sulfate evaporites are dissolving and metal sulfides are precipitating are most likely to be open space or porosity-fill textures. Ore textures and the degree of layering will depend on a number of factors including: the size of the dissolution front (interpore *vs* laminar *vs* vug *vs* solution-collapse cavern), the rate of fluid cross-flow at the interface, the degree of stability of the redox interface, and the distance the sulfate ion travels before it is reduced.

The impervious nature of any subsurface evaporite unit, even as it dissolves, means that until it is breached it is an excellent seal to migrating hydrocarbons (both liquid and gaseous). Thus the organics required for the sulfate reduction process may not only be locally derived from organic-rich sediments, they may have seeped and flowed into the interval as a hydrocarbon charge and so be trapped

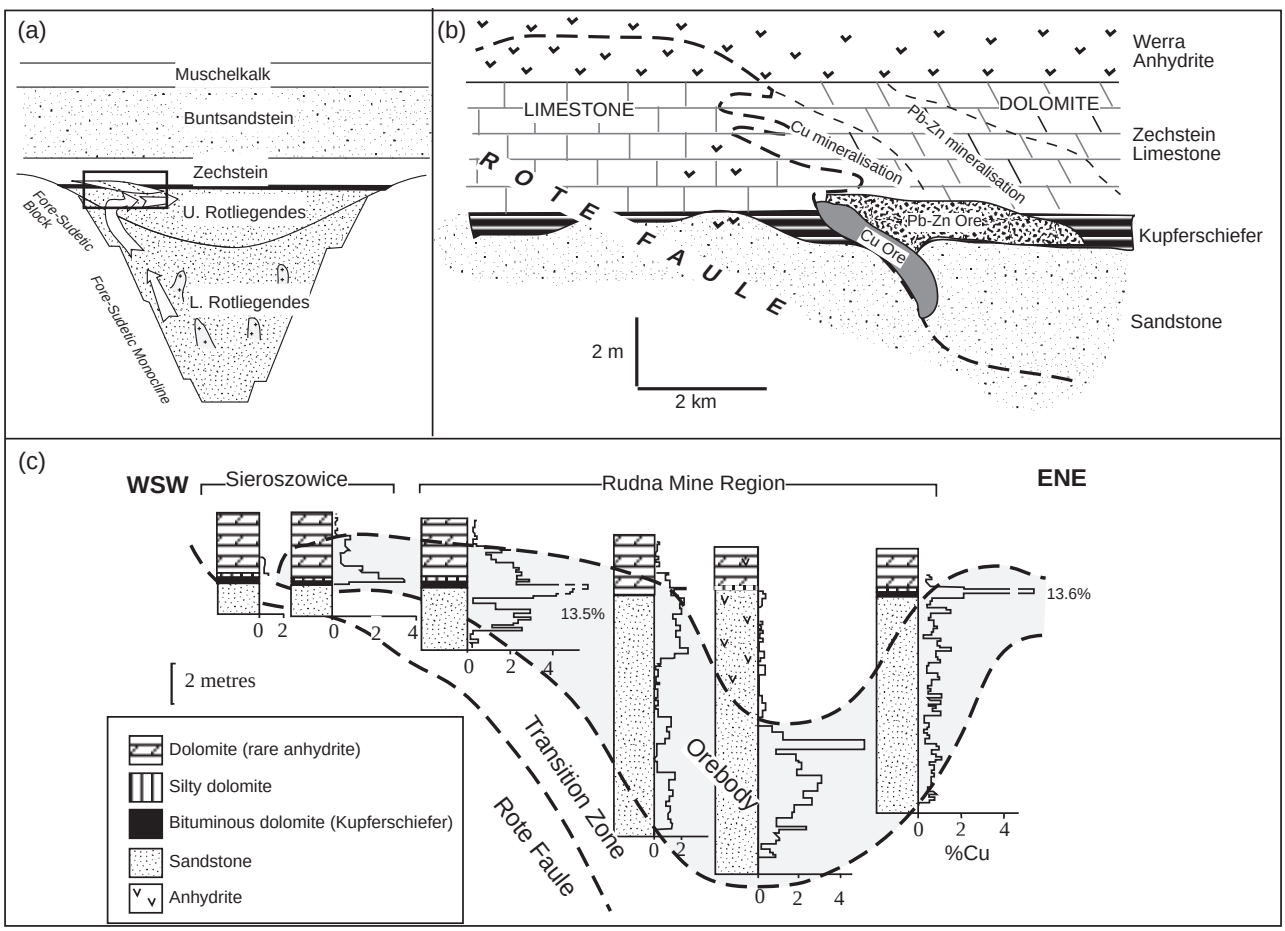

Figure 4 Rote Faule and its relation to the Kupferschiefer (modified from Jowett 1992; Vaughan *et al*. 1989; Wodzicki & Piestrzynski 1994). (a) Regional cross-section showing the focusing of the upwelling basinal water beneath the Zechstein evaporites. (b) Enlargement of region of Rote Faule [see box in (a)] showing how the mineralisation and its zonation is tied to the Rote Faule not the Kupferschiefer. (c) Distribution of Cu in the ore zone showing higher Cu enrichment (~13%) in the Kupferschiefer, but by far the greater volume of ore resides in the sandstones beneath the Zechstein evaporite seal.

directly beneath an evaporite seal. The requirement for organics in the sulfate reduction process and the ability of evaporite beds to act as a seal explain, at least in part, the ubiquitous association of sulfate evaporites, hydrocarbons/organic matter, and diagenetically created base-metal deposits.

Ores formed by thermochemical sulfate reduction and bacterial sulfate reduction can have near-identical textures; both are typically pore or vug-filling cements or evaporite replacements (Machel *et al.* 1995). One way to help differentiate the origin of the precursor H_2S is by sulfur-isotope analysis of ore sulfides that, if possible, is tied to $\delta^{13}C$ and $\delta^{18}O$ analysis of the various gangue carbonate cements and matrix that bracket the ore minerals. H_2S derived through bacterially mediated sulfate reduction tends to be isotopically light and so tends to exhibit more negative δ values (Figure 3). This is true of both the sulfur in the sulfides and of the carbon in any late-stage dolomite or calcite cements.

H_2S from thermochemical reduction is not biologically fractionated, and so $\delta^{34}S$ values of the ore sulfide tend to reflect the isotopic signature of its evaporite precursor (Worden *et al.* 1997; Emery & Robinson 1993). Limited experimental work on deeply buried anhydrite undergoing thermochemical reduction suggests that the sulfur isotopic composition of the derived H_2S is isotopically similar to, or a few per mill lighter than, the precursor anhydrite (Krouse *et al.* 1988). Thus $\delta^{34}S$ and $\delta^{13}C$ values under thermochemical sulfate reduction are much higher (more positive), while the $\delta^{18}O$ reflects elevated temperatures of late-stage diagenetic spar formation (more negative).

Isotopic distinction is not as clear-cut as it first appears; sulfur in the ore need not have come from the reduction of evaporitic sulfate, it may also come from organically derived sulfur in oil trapped in the host rock. Under this scenario, the ore has low $\delta^{34}S$ values that are similar to any associated hydrocarbons (Kesler *et al.* 1994). The range of values for these hydrocarbon systems is similar to that from bacterially mediated sulfate reduction. This overlap underlines the need for matrix characterisation, which ties stable-isotope determinations to detailed petrographic and sedimentological logs of the ore host. For example, if the ore sulfur was locally sourced, then calcite may have completely replaced the precursor anhydrite. This calcite should be sampled for carbon and oxygen isotope analyses to see if its genesis parallels that of any ore sulfides. In addition, even though sulfate salts no longer remain, the 'salt that was' textures should still be present.

DIAGENETIC EVAPORITE–METAL ASSOCIATION

Many low-temperature base-metal deposits in evaporite-entraining sedimentary basins can be related to the presence of preserved evaporites or indicators of the former presence of evaporites, such as bedded and halokinetic breccias, chert nodules and other indicators of 'the evaporite that was'. Mineralisation can be subsalt, intrasalt, or suprasalt and the salt body, or its breccia, can be bedded or halokinetic. In many cases, the H_2S that causes the ore to precipitate at the redox interface is derived from bacteriogenic or thermochemical reduction of nearby evaporitic sulfate, in combination with organics supplied by hydrocarbons ponded beneath an evaporite seal. The link between evaporites and ore precipitation is either direct, with metal accumulation at the site of the present or former evaporites, or indirect, from ascending hypersaline fluids supplied from a dissolving mother salt bed by a single or a series of feeder faults. When considering salt-related base-metal deposition it is important to place the deposit with the framework of basinal fluid flow. Subsurface evaporites, both bedded and halokinetic, are important foci and sources for high-salinity brines; they play a fundamental role in fluid escape pathways and metal precipitation. Let us now look at representatives of each of these deposit styles.

Brine focusing and copper mineralisation

When sedimentary stratabound copper deposits are studied worldwide there is consistent association with: (i) underlying or adjacent metalliferous redbeds/volcaniclastics that were the source of the copper; (ii) a through-flowing chloride brine that leached and carried the copper; and (iii) a zone characterised by the presence of reductants that facilitated the fixing of the copper sulfides. Many, but not all, of these deposits also show an intimate association with evaporites (Kirkham 1989). We shall start with what is one of the largest and best studied, the Lubin (Kupferschiefer) deposit in Poland.

SHALE AND SANDSTONE-HOSTED SUBSALT Cu DEPOSITS

Kupferschiefer Cu–Ag, Lubin, Poland

Probably the best-documented example of a subsalt base-metal accumulation is the Kupferschiefer Cu–Ag deposits of Poland. Ores are hosted in Kupferschiefer shales or in adjacent aeolian sands (Weissliegende) that together make up the upper part of the Rotliegende sequence. For example, the Lubin region in Poland has estimated ore reserves of 2600 Mt at grades >2% Cu, 30–80 g Ag/t, and 0.1 g Au/t (Kirkham 1989). Mineralisation typically occurs in reduced, evaporite-capped beds at the top of a thick continental volcanic and redbed sequence that was deposited in the Permian within a continental rift basin (Figure 4a).

These stratabound Cu–Ag Kupferschiefer deposits were long considered classic examples of syngenetic mineralisation. However, detailed work in the last decade has shown that the Cu mineralisation cuts depositional boundaries. The richest intervals of mineralisation define low-angle transgressive metal zones associated with the redox edge of the diagenetic Rote Faule units (Figure 4b) (Jowett *et al.* 1987; Jowett 1992; Oszczepalski 1994; Large & Gize 1996). The overlying evaporitic Zechstein sediments enhanced and focused the precipitation of Cu, both by forming prepared ground at the time of deposition (pyritic and organic-rich evaporitic laminite host) and during diagenesis by creating a stable dissolution hydrology, which focused the greater volumes of economic mineralisation into a redox zone adjacent to the Rote Faule boundary.

Rote Faule ('red rot') actually describes a non-mineralised diagenetic zone and loosely encompasses barren red-coloured rocks typically found near high-grade ore. It describes an oxidised hematitic interval that occurs

adjacent to the reduced highly mineralised intervals. Levels of mineralisation in the Kupferschiefer adjacent to a Rote Faule interval are typically far higher than background levels in the Kupferschiefer shales not influenced by Rote Faule development (Figure 4c). Rote Faule is not formation specific and occurs in the Weissliegende, Kupferschiefer and Zechsteinkalk strata where various types of red colour have been created by the diagenetic formation of disseminated authigenic hematite and goethite (Vaughan *et al.* 1989; Wodzicki & Piestrzynski 1994). Pyrite, and the original organics of the Zechstein carbonate and the Kupferschiefer mudstones, are oxidised and largely removed in Rote Faule intervals (Oszczepalski 1989).

The development of Rote Faule intervals indicates the oxidised portion of a redox front. In Poland, it is located at the top of the thick redbed sequence that during burial dewatering was flushed by upwelling, saline, slightly oxidised, basinal waters (Figure 4a). Ore sulfides occur on the far side of this subhorizontal oxidation–reduction front. Thus Rote Faule zones outline redox interfaces centred on the outflow positions of hydrological conduits carrying ascending, slightly oxidising, basinal chloride brines, which also carried Cu, Pb and Zn. In the ore zones, the sulfides are arranged in three distinct haloes around 'Rote Faule', in the order Cu, Pb and Zn (Figure 4b, c). Thus, around and above the Rote Faule, the base metals are zoned laterally and vertically in successive mineralisation belts of chalcocite, bornite, chalcopyrite, galena and sphalerite.

Mineralisation in Kupferschiefer-style deposits transgresses depositional facies as it is tied to the Rote Faule/saline brine interface and not to the depositional pattern. Thus copper ore is not just hosted in the organic laminites of the Kupferschiefer and the Zechsteinkalk, it also occurs in parts of the Weissliegende aeolian sandstone, a unit that is exceptionally free of organics, laminites and pre-ore sulfides. To the dismay of many syngeneticists, this depositionally clean aeolian sandstone hosts half the economic Cu-sulfides in the Lubin district (Figure 4c). A likely ephemeral reductant in this sand was methane, another was authigenic anhydrite. Jowett (1992) argued that the widespread diagenetic anhydrite cements in the Weissliegende, along with the trapped methane beneath the evaporite seal, set up burial chemistries suitable for thermochemical sulfate reduction and the precipitation of

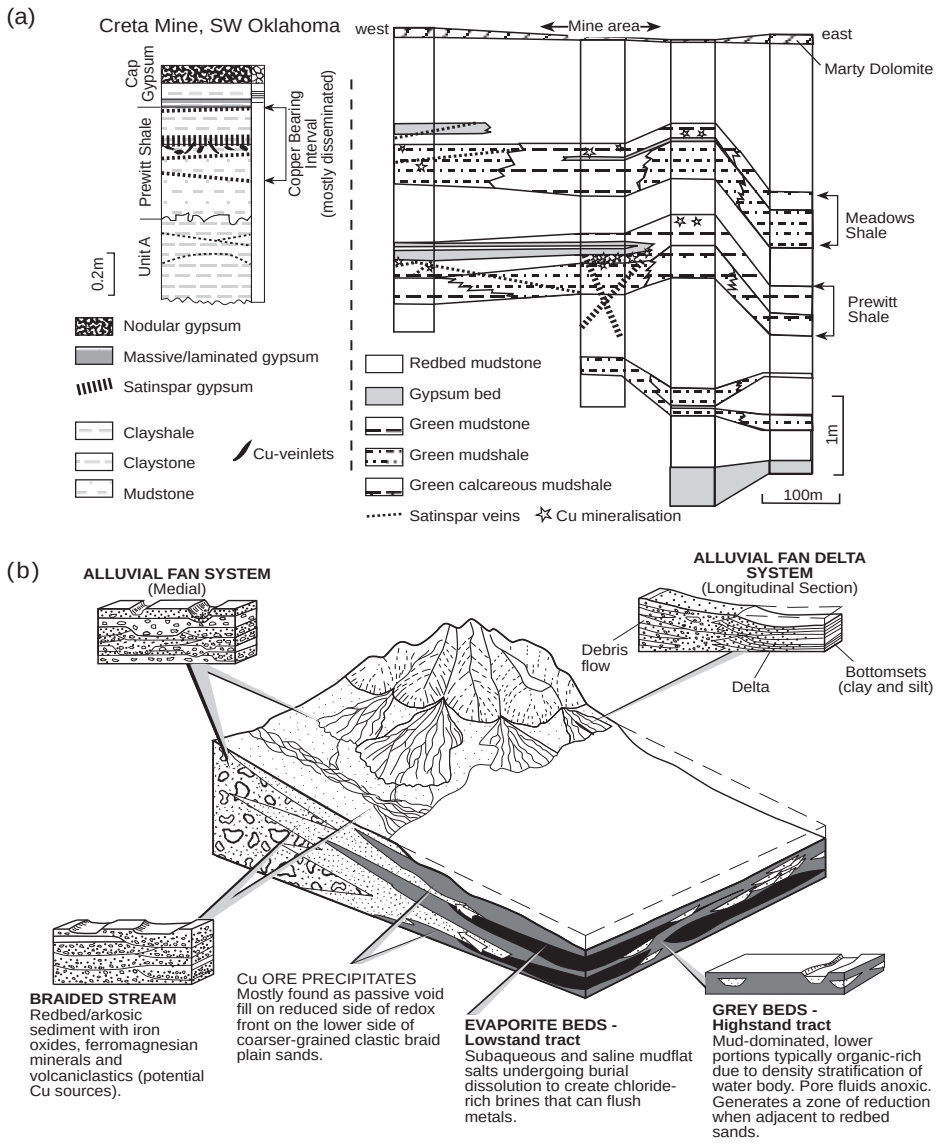

Figure 5 (a) Creta copper shale deposit, Oklahoma, showing the mineralised stratigraphy (left side of figure) and regional mine stratigraphy (right side of figure). Note the intimate association between mineralisation and evaporite indicators of former thick evaporite unit (satin-spar indicators) (after Huyck & Chorey 1991). (b) Model for the precipitation of Corocoro and other redbed/playa-associated copper ores (published with permission of JK Resources Pty Ltd).

Cu-sulfides in the Weissliegende host. As well as acting as a seal to the methane, the overlying Zechstein evaporites were also a likely source for the convectively refluxing syn-depositional brines, which first deposited the anhydrite cements.

Geometries of mineralisation suggest that the underside of the Zechstein sediments acted as a long-term seal, which ponded upwelling metal-rich slightly oxidising basinal waters within the immediately underlying Kupferschiefer or its lateral equivalents in the Weissliegende. It also acted as a pressure seal that aided hydrofracturing in the maturing organic laminates of the Kupferschiefer, as evidenced by numerous sulfide–calcite veinlets in the Kupferschiefer. An inherent lack of permeability in widespread thick evaporites also meant the upper side of the Zechstein salt beds prevented downward percolation of fresh oxygenated waters, which would otherwise have destroyed the stability of the redox interface along the underside of the dissolving salt.

A similar, but much older, example of subsalt brine-focused mineralisation is the stratiform copper deposits of the Redstone Copper Belt, Northwest Territories, Canada. It occurs along a 250 km, northwest-trending, arcuate thrust belt of Neoproterozoic (Helikian) carbonates and redbeds of the Mackenzie Mountain Supergroup (Chartrand *et al*. 1989; Ruelle 1982; Brown 1993).

SANDSTONE-HOSTED INTRASALT Cu DEPOSITS

Creta Cu deposits, Oklahoma USA

Likewise, former evaporites (now dissolution residues with satin-spar gypsum) acted as the focal point for the redox-induced precipitation of copper in the Creta deposit in the Permian Prewitt Shale of Oklahoma. Mining of the Creta deposit between 1965 and 1975 removed 1.9 Mt of copper ore averaging 2% copper, making it the second largest shale-hosted ore deposit in the United States. Lead and zinc levels are negligible at Creta. According to Huyck and Chorey (1991), the mineralisation event at Creta was early diagenetic, as indicated by: (i) copper sulfide replacing large spores and framboidal pyrite; (ii) lack of compaction of replaced spores relative to unreplaced spores; (iii) enclosure of uncompacted mud and copper sulfides by early 'matrix gypsum'; and (iv) location of the ore bed within a thick sequence of fine-grained low-permeability sediments.

The Prewitt Shale averages 2% Cu in the mine area, with a matrix composed of illite and chlorite and as much as 20% satin-spar gypsum (Huyck & Chorey 1991). It is made up of three layers: a lower blocky layer, a laminated layer and a discontinuous upper bed of impure gypsum (the 'cap gypsum'). The lowest blocky layer is a claystone to mudstone; copper, when present, occurs only in the upper 10–13 cm and is concentrated in the mudstone (Figure 5a). The overlying laminated shale, which contains as much as 4.5% Cu, includes both gypsiferous and non-gypsiferous clay-shale. Copper is concentrated in the silty laminae both in outcrop (as malachite) and in thin-section (as anilite). The cap gypsum bed directly overlies the laminated portion of the Prewitt Shale in the west, but pinches out in the east (Figure 5a). Where fully developed the cap gypsum bed (10–25 cm thick) is made up of a lower gypsum, a thin green clay-shale, and an upper gypsum.

Most published work on this deposit documents satin-spar gypsum as well as the cap gypsum, but none (including the most comprehensive work by Huyck & Chorey 1991) discuss its significance. The presence of satin-spar gypsum indicates a combination of halite solution-collapse and gypsum rehydration (Warren 1996). As such, the current forms of $CaSO_4$ in the mine area are tertiary evaporites, a result of uplift and rehydration. They were not responsible for the precipitation of the sulfides as they post-date that event. They do, however, indicate the former presence of a more substantial, but now dissolved, salt unit composed either of anhydrite, or perhaps a combination of halite and anhydrite. It was this former evaporite bed that was responsible for brine focusing and, through its dissolution, maintained a redox front that precipitated the copper sulfides.

Corocoro, northwestern Bolivia

Stratabound deposits of copper (+Ag) hosted by continental clastic sedimentary rocks occur in Central Andean intermontane basins and are known to post-date compressive deformation/uplift events in the region (Flint 1989). The deposits are relatively small and include Negra Huanusha, central Peru (Permo-Triassic); Caleta Coloso, northern Chile (Lower Cretaceous); Corocoro, northwestern Bolivia (Miocene); San Bartolo, northern Chile (Oligo-Miocene); and Yasyamayo, northwestern Argentina (Miocene–Pliocene). Sedimentary facies and host-rock diagenesis control the location of mineralisation. Deposits are irregular, elongate lenses of native metal, sulfides and their oxidation products, and are restricted to alluvial fan and playa sandstones or conglomerate facies. The Corocoro area has produced the largest amount of copper, something like 6.4 Mt of copper at a grade of 5% (Kirkham 1989).

Critical factors in ore genesis include (Flint 1989): (i) the stratigraphic association of evaporites, organic-rich lacustrine mudstone, clastic reservoir rocks, and orogenic, igneous provenance areas for both basin-fill sediments and metals; and (ii) the intrabasinal evolution of metal-mobilising saline brines from the buried and dissolving lacustrine evaporites and mudstone-derived reducing fluids. The same diagenetic fluids also caused the dissolution of early, framework-supporting cement in the host clastic sedimentary rocks (Figure 5b). Ore minerals (including native copper) are secondary cement fills within secondary intergranular pores created by the dissolution of earlier carbonate and sulfate cements. The ore-hosting clastics lie within the Vetas Member of the Ramos Formation and were deposited as redbeds in braidplains or fluviodeltaic playas about the margins of saline evaporitic lakes (Flint 1989). Abundant evaporites are still present in the Ramos Member at Corocoro.

The playa depositional environment in combination with the burial evolution of the adjacent evaporites controlled the formation, transport and precipitation of the copper ore. Playa sandstones, sealed between impervious evaporitic mudstones, created the plumbing for focused metalliferous fluid migration toward the basin margin. It appears that the carbonaceous material at Corocoro was

concentrated in the sandstones and conglomerates and not in the shalier members of the sedimentary sequence (Eugster 1989). The organics entrained as plant matter in the sandstones, along with those migrating as hydrocarbons out of the basin, created locally reducing pore environments. This in combination with sulfur supplied as H_2S from the adjacent dissolving calcium sulfate beds, as well as from dissolving intergranular sulfate cements, precipitated copper in the newly created secondary porosity. The pore-water chemistry and flow hydrology of this sandstone-hosted Cu system shows many affinities with diagenetic uranium-redox precipitating systems.

SANDSTONE-HOSTED Cu IN A SUPRASALT POSITION

Copper emplacement in a suprasalt position often reflects brine focusing atop halokinetic salt where the escaping metalliferous brines move along fault or brine gradients generated by the flowing and dissolving salt unit.

Dzhezkazgan Copper, Kazakhstan

A classic sandstone-hosted Cu deposit in a suprasalt position is the large Dzhezkazgan copper deposit located at the northern edge of the Chu-Saysu basin, Kazakhstan. Copper mineralisation is hosted in middle to Upper Carboniferous continental successions of conglomerate, sandstone, shale and evaporites (Gablina 1981, 1997; Susura *et al*. 1986). Reserves estimated for this deposit, but based on questionable data, are 400 Mt with a copper grade of 1.5% (Kirkham 1989). The depositional setting of the host was an intermontane closed-basin, which was made up of deltaic–lagoonal, alluvial and saline lake sediments. Hosts to the ore are siliciclastic redbeds that are laterally equivalent to bedded evaporites and underlain by Lower Carboniferous organic-rich sediments (presumed source rock) and sealed by shaly carbonates. The main copper sulfide and pyrite orebodies occur in an anticlinal trap located along the flanks of a basement high, and sit atop a salt ridge (Figure 6a). The host redbed sandstones become more evaporitic basinward and coarser grained toward a pinchout along the basement highs. The mineralised sandstone is pyritic, with reduced pore fluids created by entrained hydrocarbons and high salinities. In contrast, the interbedded shales are red due to more oxidising pore fluids. These redbeds were in part derived from continental volcanics.

Gablina (1981) suggested that an early salt dome with crestal erosion developed in the marine rocks and lowermost redbeds that overlie the salt anticline. Bed geometries

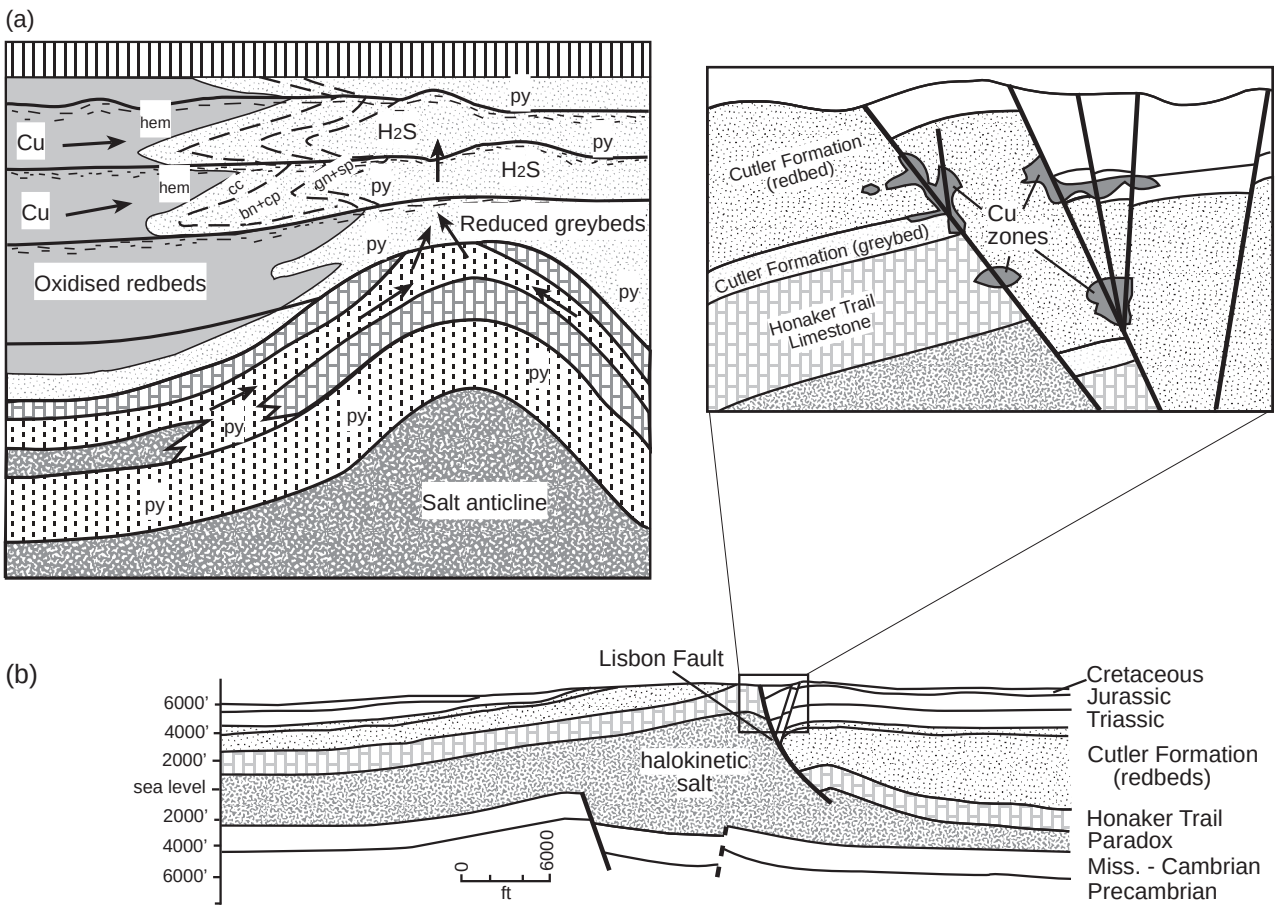

Figure 6 (a) Schematic cross-section of the Dzhezkazgan deposit showing Cu deposition controlled by the halokinetically controlled redox interface. hem, hematite; cc, chalcocite; bn, bornite; cp, chalcopyrite; gn, galena; sp, sphalerite; py, pyrite (after Kirkham 1989). Note the similarity of the Cu and Pb–Zn zonation to that in the Rote Faule in Figure 4b. (b) Copper in the Lisbon Valley, Utah showing copper precipitation in the fault-segmented crestal position of the Lisbon Valley salt anticline (after Morrison & Parry 1986; Kirkham 1989).

illustrated in Figure 6a suggest the bed thinning and truncation were induced by halotectonics. The domal structure focused the flow of reduced hydrocarbon- and H_2S-bearing formation waters into a vertically ascending plume of escaping compactional waters. Extensive precipitation of copper and other metals occurred at the regional redox front between the ascending evaporite-focused plume and Cu-bearing waters from adjacent redbeds. In this case the role of the dissolving catabaric evaporites was to supply reduced brines and to create a focus atop a halokinetically controlled salt anticline. The precipitation mechanism and the metal zonation are the same as in the Kupferschiefer model, but in this case, the relative position of the evaporite and the redbeds are reversed. The main evaporite bed lies below the redbeds, which are the ultimate source of the metals. Although the mineralised beds are stratabound, this deposit is really a result of brine focusing due to halokinesis.

Lisbon Valley Cu(±Ag), USA

A similar, but less economically significant, analogue is to be found in the Lisbon Valley, USA, where Cu(±Ag) ores occur along extensional faults, controlled by salt anticlines (Figure 6b). The ore is hosted in redbed sediments of the Paradox Basin and in the coal-bearing horizons of the overlying Cretaceous Dakota Sandstone in southeast Utah and southwest Colorado (Morrison & Parry 1986). Cu is found as vein fillings, sandstone pore fillings, and as replacement of coalified plant fossils. The deposits are clearly related to halokinetically induced faults, and have not been offset by post-mid-Cretaceous movements (Figure 6b). The largest deposits, Big Indian and Blackbird, occur along the Lisbon Valley Fault in coal-forming horizons of the Cretaceous Dakota Formation. Almost all the mineable copper ore occurs within several hundred metres of either the Lisbon Valley Fault or major fracture zones.

Fluid inclusions, mineral chemistry, and C-O stable isotopes in calcite gangue associated with Cu ores at Lisbon Valley suggest they formed through subsurface mixing of two diagenetic waters. Fluid temperatures ranged from 72 to 103°C, while salinities were 5 to 20 equiv. wt% NaCl during calcite deposition (Morrison & Parry 1986). Cu-bearing, saline, basinal fluids migrated up along fault zones, and upon mixing with shallower reduced Ba-rich groundwater deposited ore and gangue minerals. A combination of dilution and reduction of upwelling basinal brines induced mineral precipitation. The metal-carrying fluid probably originated in the redbed aquifers of the Permian Cutler Formation. The brines may have equilibrated for long periods in these Cutler Formation aquifers and only been released during faulting and halokinetic activity driven by the Late Cretaceous – Early Tertiary Laramide Orogeny. Then faults, such as the Lisbon Valley Fault, breached the redbed aquifer and so allowed pressurised, heated metalliferous fluids to escape upward along the faults until they encountered permeable units replete with reductants, such as occurred in the Dakota and Wingate Sandstones (Kirkham 1989).

In my opinion, the role of flowing salt in driving and focusing the flow of metalliferous brines has not been given the importance it deserves in the explanation of mineralisation in a Lisbon Valley-style deposit. The style of faulting that focuses the mineralisation is a response to movement on the underlying salt structure (Figure 6b). The dissolution of this underlying salt also supplied the chloride-rich brines that leached the metals from adjacent redbeds. It also created the thermal and brine density contrasts that drove the convection and metal enrichment of this brine. Without halokinesis and salt dissolution there would be no focusing into this structurally controlled deposit. Nor would there be any long-term maintenance of the redox haloes about the faults that allowed this deposit to accumulate. Without the underlying halokinetic salt, economic levels of copper sulfides simply would not be there.

Dongchuan and Lianong Cu, China

Suprasalt stratabound sediment-hosted copper deposits, associated with a widespread halokinetic breccia unit, are found in a 450 km-long rift in the Yunnan Province of China (Huichi *et al.* 1991). The Dongchuan area is the largest of five copper mining areas in this north-trending rift, which contains sandstone, shale, and carbonate rocks of the Kunyang Group of Mesoproterozoic age. Deposits in the area range from 10 to 100 Mt of ore with ore grades of 1 to 1.5%. Three formations, about 1200 m thick, in the lower part of the group contain the copper deposits. They are from bottom to top: the Heishan Formation, mainly a carbonaceous slate; the Laoxue Formation, mainly a stromatolitic dolostone; and the Yinmin Formation, chiefly purple slate and sandstone. Mafic igneous rocks intruded these formations. Below the Yinmin Formation is a thick breccia consisting of clasts of Yinmin-type shale and sandstone, dolerite, and other rocks. The three ore-producing formations and the breccia are exposed in a band of steeply dipping strata extending across the Dongchuan area.

Most of the copper ore occurs in the lowermost dolostones of the Laoxue Formation. Vein-type orebodies account for only 3% of the total ore reserves in the area. Stratabound ores characteristically occur as disseminations of sulfides along stromatolitic algal layers. Locally, high-grade vein-type ores cross-cut the dolostone. Both ore types contain bornite, chalcopyrite, chalcocite, and other minerals. Fluid inclusions in quartz veinlets contemporaneous with the copper mineralisation contain liquid, vapour and daughter minerals: NaCl, $CaCl_2$, KCl and $BaCl_2$. They homogenise between 200 and 280°C (Huichi *et al.* 1991).

The breccia was produced by tectonically induced salt diapirs from which the salt was later removed by hydrothermal leaching. Copper ores are associated with the thermal anomaly that resulted from this salt diapirism and was contemporaneous with dolerite intrusion (Huichi *et al.* 1991; Wu & Xiji 1981). Hot brines circulating upward along the flanks of the diapir leached copper from the oxidised Yinmin Formation and carried it to the base of the overlying Laoxue Formation. Sulfide-rich fluids were formed by reaction of evaporite sulfates with decayed organic matter in the dolostones. Copper sulfide deposition in the dolostones resulted from the mixing of these fluids. Continued circulation leached all of the remaining salt from the diapir,

and the overlying and surrounding rocks collapsed to form the breccia. Texturally, these halokinetic breccias are very similar to the diapiric breccias that are widely exposed in the Flinders Ranges, South Australia and the Amadeus Basin of central Australia.

Another Proterozoic example of the focusing effects of the peridiapiric setting is clearly illustrated in Palaeoproterozoic Fe–Cu sulphide deposits, eastern Liaoning, northeastern China (Wang *et al.* 1998). This area lies within the same region as the meta-evaporite borate deposits described in Peng and Palmer (1995). The sulfides were precipitated at two sites: as breccias, lenses, and veins around venting centres; and as stratabound pyrite–chalcopyrite, which are associated with anhydrite located distal to the salt domes. Within each mining district the proximal ores are associated with brecciated, albite- and tourmaline-rich metasediments. The sulfides in the proximal ores have $\delta^{34}S$ values of 8.9 to 12.7‰, whereas the distal ores have $\delta^{34}S$ values of 2.6 to 8.8‰ for the sulfides and 7.9 to 19.0‰ for the anhydrite; suggesting a sulfate-dominated sulfur source, with the pyrite $\delta^{34}S$ variations arising mainly from decreasing temperatures away from the centres of the deposits. According to Wang *et al.* (1998) a model in which sulfate–carbonate rocks were deposited in peridiapir sinks during salt diapirism best describes the origin of the deposits. The salt domes then acted as foci for subsequent hydrothermal venting of chloride-rich metalliferous fluids and the adjacent peridiapir sediments became the centres of sulfide mineralisation. The sulfides precipitated during interaction of the reduced, metal-bearing hydrothermal fluids with the *in situ* sulfates, which acted as the major *in situ* source of evaporitic sulfur.

Brine focusing and sulfate-facilitated fixing of Pb–Zn

As we have seen for evaporite-associated copper deposits, the upward escape of subsalt basinal brines is typically focused along the underside of thick basinwide evaporite

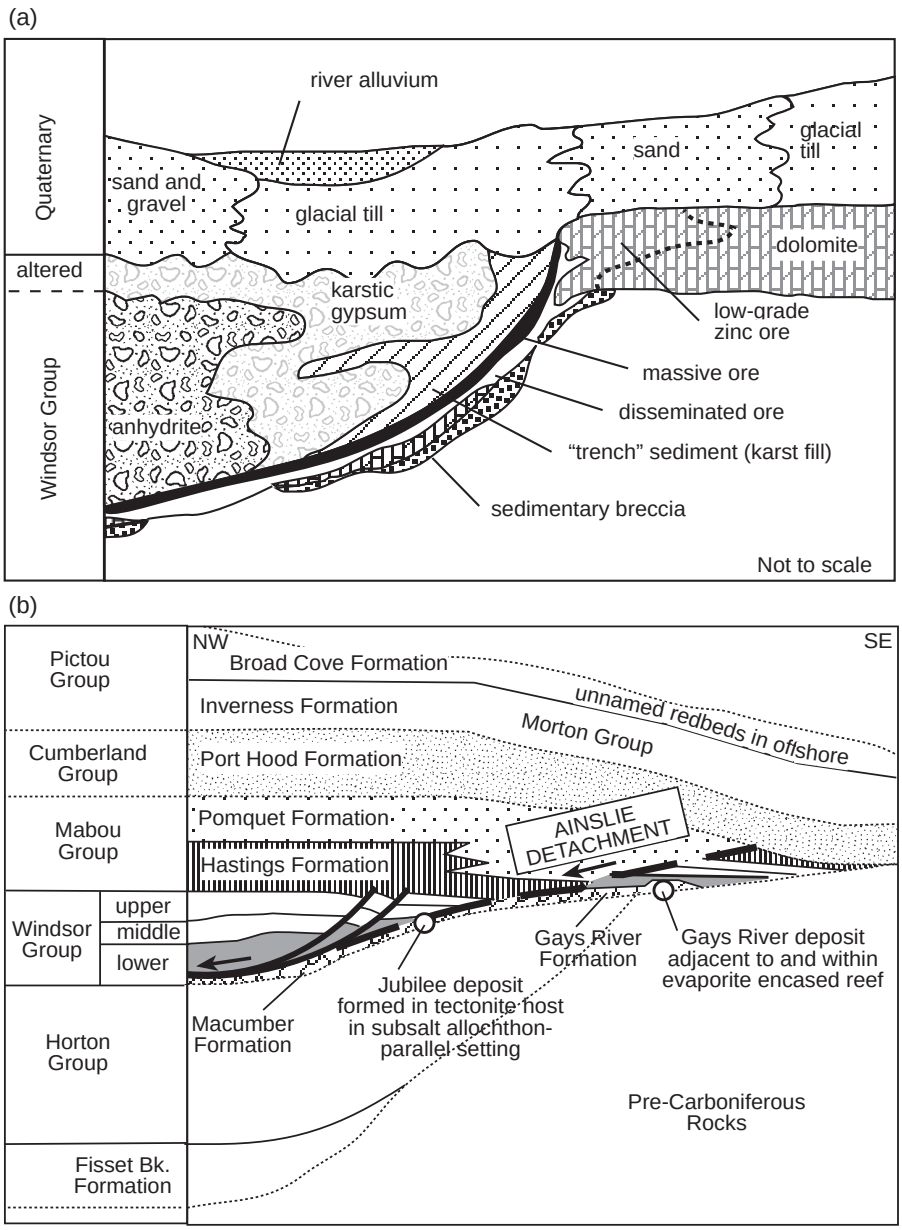

Figure 7 (a) Cross-section of the Gays River deposit, Nova Scotia showing intimate association between the dissolved evaporite underbelly and the position of the massive Pb–Zn ore (after Kontak *et al.* 1994). (b) Schematic cross-section of the stratigraphy and position of the regional Ainslie Detachment, in Nova Scotia, a major allochthon feature associated with salt flow and gravity gliding into the basin. Lubricating evaporites of the lower Windsor Group (Carrols Corner Formation) are shaded grey. Note the salt raft tectonics geometry with thickening of the Mabou Group in the salt-withdrawal sink. Jubilee-style deposits are hosted in the salt tectonites created by the detachment. In contrast, the Gays River-style of deposit is formed at the evaporite-encased underbelly contact adjacent to the salt-encased reefal buildup. In the case of the Jubilee deposit it was focused by the feather edge of the salt unit (after Lynch *et al.* 1998).

units and can only escape into overlying strata at breach points in this salt body. Such breach points may be the feather-edge of the evaporite bed or extensional faults that cross-cut the flowing and deforming salt body. Some of these faults may be induced by the basinward flow of salt; others may be large regional basin-defining structures. Any dissolving sulfate units that lie atop the dissolving halite bed that is supplying the brine carrier, and are in the passageway of this upward escaping chloride-rich metalliferous brine, can act as suppliers of sulfur. In conjunction with trapped hydrocarbons, these sulfate beds can create redox interfaces suitable for the precipitation of lead–zinc ores. As with copper, these redox fronts can occur in subsalt, intrasalt and suprasalt positions. Many of the carbonate-hosted Pb–Zn deposits within this context have been be classified as Mississippi Valley Type deposits (MVT), but the following discussion does not use this terminology, rather it looks at Pb–Zn mineralisation in the context of subsalt, intrasalt and suprasalt base-metal accumulations.

There are many sedimentological studies of Zn–Pb deposits that argue for, or allude to, the presence of evaporites as the probable source of sulfur in the metal sulfides (Fontboté & Gorzawski 1990; Ghazban *et al*. 1990; Warren & Kempton 1997). Typically in such orebodies all that remains of the former evaporites are dissolution breccias or other indirect indications of vanished evaporites ('the salt that was'). Zn–Pb deposits associated with bedded evaporites generally occur in dolomitised shelf carbonates or sandstones that are adjacent to, or within, feeder faults. Such systems are sometimes located at or near the high-energy depositional shelf edge, as defined by the rock matrix character of the host, or are located adjacent to the dissolution edge of the focusing evaporite. In many deposits, such as Gays River, Jubilee, Cadjebut or San Vicente, the two features may coincide.

SUBSALT BRINE FOCUSING

As in the subsalt copper deposits, the role of the salt was probably that of focusing the upward escape of Pb–Zn-rich metalliferous brines. However, when these brines encountered a calcium sulfate bed that was undergoing dissolution and thermochemical sulfate reduction the metals were precipitated as sulfides dominated by sphalerite and galena. The sulfate may have been present as: (i) a basal anhydrite to the dissolving salt bed—a subsalt position (possibly a diagenetic unit: El Tabakh *et al*. 1998; Warren 1999); or (ii) as intrasalt replacements of platform sulfate beds, which were located at or near where such beds intersected regional faults, which in turn were acting as brine conduits, as in the Cadjebut and San Vicente deposits.

Gays River and Jubilee Zn–Pb

The Gays River and Jubilee Zn–Pb deposits in southern Nova Scotia, Canada, represent well-studied examples of the confluent style of salt-focused subsalt mineralisation. Gays River has reserves ~2.4 Mt at 8.6% Zn and 6.3% Pb of either massive or disseminated ore (Figure 7a) (Kontak *et al*. 1994; Kontak & Jackson 1995; Sangster *et al*. 1998). The Jubilee deposit extends over 2.75 km^2, and contains 0.9 Mt of 5.2% Zn and 1.4% Pb, and is hosted in the laminated limestones and salt tectonic breccias of Macumber Formation (basal Windsor Group: Fallara *et al*. 1998). Both are hosted by Windsor Group (Visean) carbonate/evaporites that were deposited in several evaporitic sub-basins of the larger Maritimes Basin of eastern Canada. They are two of the many lead and zinc prospects found in Lower Carboniferous limestones of the Maritime region, eastern Canada (Armstrong *et al*. 1993).

At Gays River, it was the adjacent dissolving and sealing anhydrite unit along with associated entrapped hydrocarbons, and not the adjacent permeable dolomitised carbonate buildup, which controlled the locality and the process of mineralisation. The massive ore adjacent to the sulfate–evaporite bed is made up of fine-grained, beige coloured sphalerite and medium- to coarse-grained galena. Massive ore is only found along the carbonate–evaporite contact (Figure 7a). Disseminated ore occurs adjacent to the massive ore or its evaporite seal and is hosted by Viseanage, dolomitised carbonate rocks (bank and interbank facies) that are part of a series of carbonate banks (i.e. the Gays River Formation). The main ore-hosting authigenic dolomite replaced its limestone precursor prior to the mineralisation event (Savard 1996). Dolomitisation played a role in ground preparation, but was not directly tied to the Zn- and Pb-rich basinal fluids that mineralised the Gays River deposit.

The presence of massive ore at the carbonate–evaporite (anhydrite) contact shows the focusing effect of the impervious evaporites, and that the basal anhydrite along the underside of the thick evaporite package was probably the major source of sulfur. It is highly likely that the evaporites which once covered the Gays River carbonate buildup formed a regional seal at the time of ore emplacement. It allowed mineralising solutions and associated hydrocarbons to pond at the contact with the permeable dolomite host rocks beneath it (Figure 7a). The evaporite–carbonate interface focused the mineralisation, not the dolomitising of the matrix. The dolomitised carbonate's main role was that of passive host to the mixing of mineralising solutions, entrained hydrocarbons, and the thermochemically reduced sulfur derived from the dissolving evaporites.

At Jubilee, transitional interstratified limestone and anhydrite overlie a laminated limestone, with a massive anhydrite unit capping the sequence. This ore-hosting Macumber Formation is the lateral equivalent to the Gays River Formation that hosts the Gays River deposit (Figure 7b). The Macumber Formation is made up of three main lithofacies: (i) a micritic lithofacies that locally contains ooids, oncolites and pellets; (ii) a finely laminated lithofacies; and (iii) a mineralised breccia facies (Fallara *et al*. 1998). The facies transition between the first two lithofacies is gradational and concordant, whereas the contact between the finely laminated lithofacies and the mineralised breccia is sharp. The breccia is conformable at the top of the Macumber Formation and never cross-cuts it (Figure 7b). The deposit is located near two faults interpreted by Hein *et al*. (1991) as normal synsedimentary faults. Armstrong *et al*. (1993) suggested the mineralisation was a low-temperature sulfide system related to the former presence of hydrocarbons. Overlying the breccia at the base of the Carrols Corner Formation is a transitional zone of

interbedded limestone and evaporite. It passes up into the Carrols Corner Formation, a thick sequence of anhydrite and gypsum up to 300 m thick, and passes down dip into thick halite-dominated successions (unit shown in grey in Figure 7b).

Breccia that hosts the Jubilee ore has been interpreted as: (i) an evaporite solution collapse breccia; (ii) a tectonic breccia that was the result of normal faulting and magmatic intrusions that created a horst structure; and (iii) a collapse breccia produced by the subsurface dissolution of evaporite during the circulation of the mineralising fluid. Recent work on breccias in the lower part of the Windsor Group by Lavoie *et al*. (1998) has shown that all three origins are correct. What previously was loosely called the Pembroke Breccia, and considered a single unit, does in part host the ore. The problem is that the Pembroke Breccia is a term that is used to describe all breccias in the region, when in reality it does not describe a single lithofacies or a formation-specific unit. Rather, the term Pembroke Breccia has been applied to three temporally and genetically distinct breccia bodies. There is a pre-ore synsedimentary carbonate slope breccia, a syn-ore tectonic breccia related to the Ainslie Detachment, and a modern karstic post-ore evaporite solution collapse breccia related to the modern groundwater system. The formation of the syn-ore breccia was aided by pressure buildup and hydrofracturing beneath the regional evaporite cap, processes that also facilitated the formation of the regional subsalt detachment (Ainslie Detachment; see below).

The Gays River and Jubilee deposits are part of a larger regional scale Zn–Pb–baryte–evaporite association related to evaporite-focused outflow interfaces during dewatering and salt flow in the various sub-basins of the Maritimes Basin of eastern Canada (Lynch *et al*. 1998). Regional isotope and inclusion studies, summarised by Ravenhurst *et al*. (1987), show the deposits all formed from basinal brines, which were derived from >5 km depths in catabaric sediments that lay beneath the Visean evaporites. These sets of deposits are useful analogues for the genesis of the halokinetically controlled Neoproterozoic baryte and sulfide deposits in the Flinders Ranges, South Australia.

The regional detachment surface, known as the Ainslie Detachment, was probably created by lateral 'into-the-basin' gravity sliding or displacement along the sole of the regional salt unit, which characterises the lower Windsor Group (350 m+ evaporites of the Carrols Corner Formation). Its underside focused the flow of escaping metalliferous brines, which migrated laterally through the Tournaisian clastic rocks and the immediately overlying tectonic breccia. Brines then escaped and mixed with shallower basinal fluids at breach points in the evaporite aquiclude about the basin margin (Figure 7b) (Lynch *et al*. 1998; Lynch & Keller 1998). Thermochemical sulfate reduction was the main metal-fixing reaction of the various deposits, with the sulfur/sulfate supplied by the adjacent evaporites and the organics from the migrating hydrocarbons (Armstrong *et al*. 1993).

The salt tectonic style that characterises the main offshore basin is similar to the raft tectonic styles that typify other salt-floored passive margins such as the Gulf of Mexico and offshore Brazil (Warren 1999 chapter 5). The interrelationships between metalliferous brines, allochthons and notions of raft tectonics creating breach points in a salt seal (allowing the escape/reduction of metalliferous chloride brines) are discussed further below and used to define an allochthon-associated sedex model.

INTRASALT Pb–Zn DEPOSITION

Pb–Zn at Cadjebut, Australia and San Vicente, South America

Cadjebut in the Canning Basin and San Vicente in South America are Pb–Zn deposits created by fault-associated focusing of escaping basinal brines into zones where sulfate-rich evaporite beds are being replaced by sphalerite and galena. Brine-focused outflow in the Canning Basin is today beneath basinal shales rather than directly beneath a deeply buried basin-wide salt. These basinal brines probably had their metal-carrying capacity increased by the dissolution of more deeply buried and older basin-wide salts such as still occur in association with redbeds located further out in the Canning Basin (e.g. Ordovician–Silurian Mallowa Salt: Cathro *et al*. 1991). However, this regional basin hydrology did not fix metal sulfides in either basin. Rather, it was the occurrence of the sulfate evaporites in the platform margin in positions where these beds encountered metalliferous chloride-rich brines ascending large basin-margin defining growth faults.

Across the Cadjebut region a number of beds of calcium sulfate evaporites, and their lateral dissolutional equivalents, have been cored in the Devonian Lower Dolomite Member (Warren & Kempton 1997). Their lateral equivalents in the immediate vicinity of the mine are evaporite solution breccias (rock matrix breccias) that in turn are the lateral equivalents of the ore zones (Figure 8a). The deposit undoubtedly represents the *in situ* replacement of a number of evaporite beds by Pb–Zn sulfides on a one-for-one basis. Isotopic evidence clearly shows the metal-fixing process was thermochemical sulfate reduction. At the stratigraphic level of the evaporites, the sulfate to sulfide replacement process occurred across centimetre- to metre-sized cavities, and so the banded and breccia replacement textures are layered, sometimes forming 'zebra' textures. A cavity-infill replacement process means that the ore textures are not necessarily a direct mimicry of the precursor laminar to nodular evaporite textures (Tompkins *et al*. 1994 *vs* Warren & Kempton 1997). For a more complete discussion of Cadjebut, its formative fluids and its surrounds the interested reader is referred to Arne (1996); Tompkins *et al*. (1994); Warren and Kempton (1997) and references therein.

The San Vicente Zn–Pb ore deposit is situated 300 km east of Lima, in central Peru, in the Upper Triassic – Lower Jurassic carbonate platform (Pucara Group) at the western margin of the Brazilian Shield (Fontboté & Gorzawski 1990). Sphalerite and galena, the only ore minerals, occur as lens-shaped bodies generally parallel to the bedding. The three ore-bearing dolomites lie within the 1400 m-thick Pucará sequence (Figure 8b). The San Vicente dolomite is the main ore-bearing unit and hosts the exploited part of the San Vicente mine. Other ore occurrences are located in the San Judas Dolomite and the Alfonso Dolomite.

Individual ore lenses are in dolomitised tidal flat and lagoon facies characterised by cryptalgal laminae and evaporite moulds after former sulfate evaporites (including gypsum). As in Cadjebut, there is a direct relationship between the occurrence of former evaporite layers and ore lenses implying that the sulfate evaporites were the source of sulfur in the mineralised lenses.

Strontium, carbon, oxygen and sulfur isotope geochemistry was carried out on consecutive crystallisation generations in the San Vicente region (Spangenberg *et al*. 1996; Moritz *et al*. 1996). The results obtained display systematic trends that all show the San Vicente lead–zinc deposit formed during burial diagenesis by the mixing of incoming hot saline, slightly acidic, radiogenic (Pb, Sr) basinal fluids and local sulfate-rich formation waters derived by the dissolution of sulfate evaporites. The temperatures indicated by sulfur isotope geothermometry (75–92°C) are consistent with temperatures reached at a burial depth of ~2–3 km. Such burial depths were probably reached by the end of the Jurassic. The ores were emplaced by the thermochemical reduction of evaporite-derived sulfates, at or near the ore site, and by the introduction of a zinc- and lead-bearing basinal brine into the same zone (Fontboté & Gorzawski 1990).

ALLOCHTHON AND LAMINITE MINERALISATION

For many years, salt diapirs have been viewed as potential targets for petroleum, salt and sulfur. Only in the last decade, in a wider context of rapidly evolving models of salt allochthons, have individual diapir structures also come to be viewed as potential targets for Cu, Pb and Zn exploration (Wang *et al*. 1998). This section of the review enlarges these notions of diapir-associated mineralisation to encompass the more regional effects of salt flow and salt allochthon emplacement.

A salt allochthon is a sheet of flowing salt that may deform and flow into salt pillows and diapirs at the same stratigraphic levels as the mother salt bed, or it may be emplaced as a series of mobile and deforming sheets into successively higher tiers in the stratigraphy. Allochthonous salt sheets typically overlie younger strata as flowing salt beds and are typically no longer connected to the mother salt bed, yet they have areas measured in hundreds of square kilometres and thicknesses of up to several kilometres (Warren 1999 chapter 5 for a detailed discussion of salt allochthons). In contrast, a salt structure that extends several kilometres vertically down to the mother salt bed is described as autochthonous salt. Geometries of salt flow

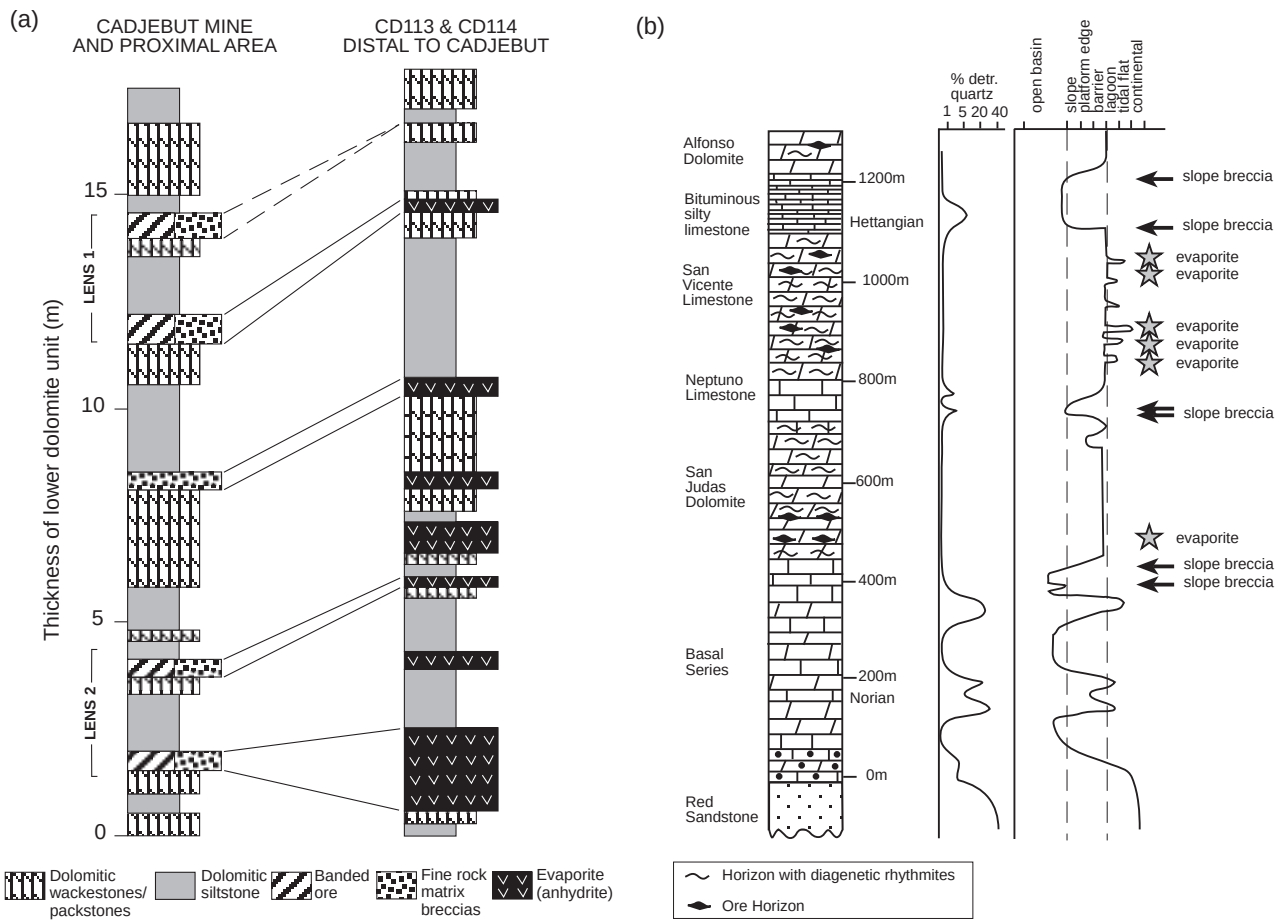

Figure 8 (a) Stratigraphy in the Cadjebut mine region, Canning Basin margin, Australia. Note the correlation of the ore lenses in the mine to evaporite solution breccias in the immediate vicinity of the mine and ties to preserved sulfate evaporite beds distal to the mine (after Warren & Kempton 1997). (b) Stratigraphic sequence in the San Vicente Mine, central Peru (after Fontboté & Gorzawski 1990). Note the close association of evaporite occurrence and base-metal mineralisation via thermochemical sulfate reduction.

or allochthon traces are controlled by the efficiency of salt evacuation as the salt pod flows to the surface leaving behind evidence of its passage as a series of welds (Figure 9a). When salt evacuation is efficient, the result is a large counter-regional suture or salt weld. When less efficient a regular series of salt residuals or rollers are left behind (that may later collapse to form salt solution breccias) to form a roho system. As salt is evacuated, the overburden may touch down on the salt underburden to form a salt weld. After the salt is evacuated where there has been movement across the weld, it forms a fault weld. The salt weld may occur at the stratigraphic level of the original salt deposit or mother salt bed, where it forms a primary weld, or at higher levels in the stratigraphy (secondary weld). Before they are dissolved, the salt tongues may flow kilometres vertically and tens of kilometres laterally.

Secondary allochthonous tongues or tiers can be surrounded and encased in normal marine sediments, not the evaporite-associated sediments that typify the level of the primary layer or weld. When the salt tongue lies near the sea floor as a salt glacier (namakier) it typically forms a topographic high on the sea floor that is covered by a thin carapace of marine sediment. Owing to the inherent instability of this carapace it is periodically shed and slumped into the adjacent low, which is often a sea-floor brine lake filled with anoxic hypersaline brines.

Mineralised systems associated with salt allochthons can be divided into three types: (i) caprock-hosted deposits, where the host rock consists of anhydrite and bacteriogenic limestone (Figure 9b); (ii) peri-allochthon deposits, where the bulk of the mineralisation resides in a laminar organic-rich sediment host adjacent to the allochthon or diapir crest (Figure 9c); and (iii) fault-associated mineralisation that lies above the salt/halokinetic breccia, where the same faults that were created during synkinematic salt flow also channelled the mineralisation (e.g. Lisbon Valley style deposits: Figure 6b). All styles of mineralisation can occur in a single salt province, and the relationships can be preserved well into the metamorphic realm (e.g. Kipushi style: see Warren 1999 for summary).

Caprock-hosted Pb–Zn deposits, Gulf Coast and North Africa

Relatively small deposits of Pb–Zn with a diapir association were recognised in northern Africa more than 100 years ago, but it was not until the geology of diapir-hosted subeconomic deposits in the Gulf of Mexico (Kyle 1991) and

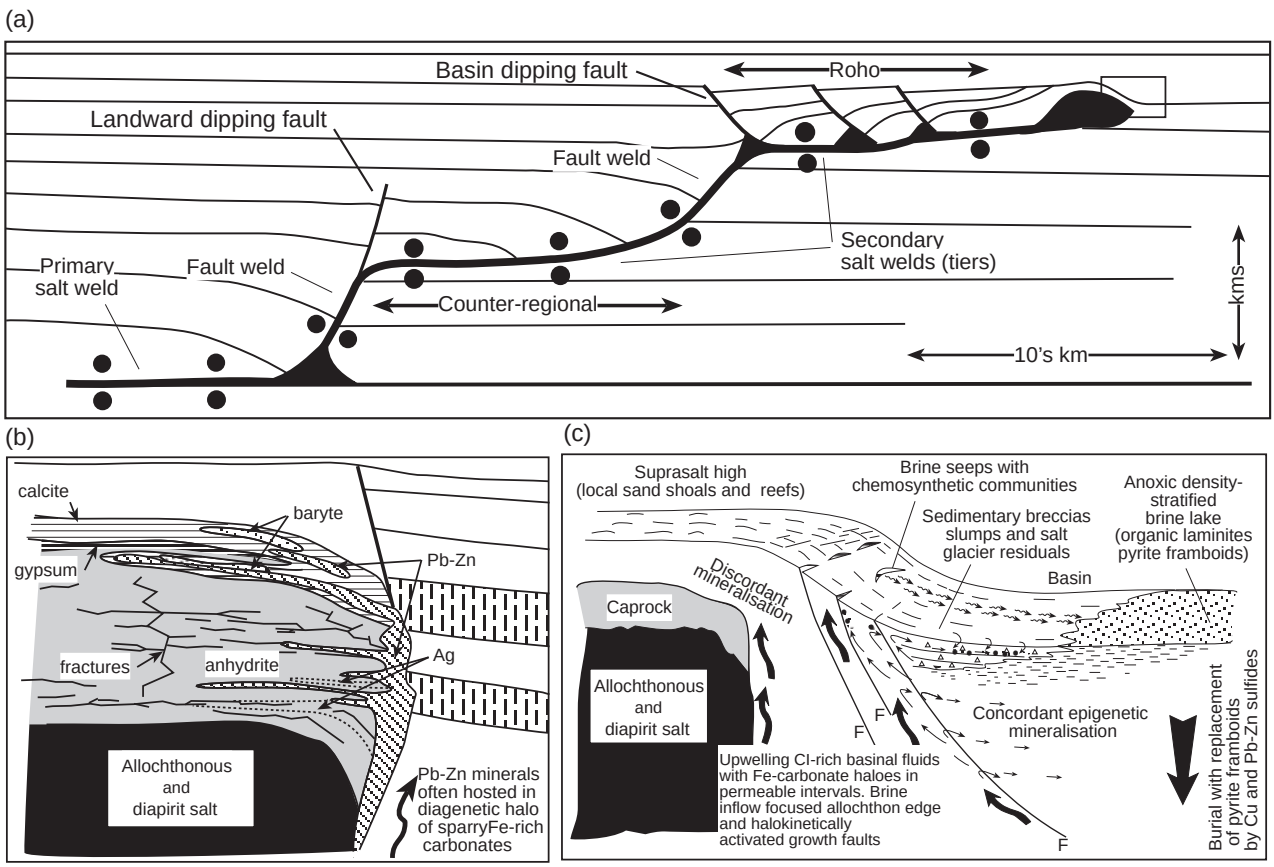

Figure 9 Salt allochthons and base-metal mineralisation. (a) Geometries of salt flow or allochthon traces are controlled by the efficiency of salt evacuation (after Jackson *et al.* 1994; Rowan 1995). When the mother salt bed completely dissolves or flows away it leaves behind a primary salt weld; remnants of salt tiers higher in the stratigraphy are called secondary salt welds. Where the passage of a salt allochthon has facilitated faulting it leaves behind a salt weld that is also called a fault weld. (b) Patterns of mineralisation in a caprock (after Price *et al.* 1983). (c) Model of peri-allochthon mineralisation. Note the similarity of the brine outflow hydrology to that in classic sedex-style systems (published with permission of JK Resources Pty Ltd).

economic north African diapir- and peridiapir-hosted deposits, such as Bou Grine (Rouvier *et al.* 1985; Orgeval 1991), were understood that the significance of salt flow in controlling this style of Pb–Zn was fully appreciated. Mineralogically, the diapir-associated mineral deposits are similar to many other carbonate- and shale-hosted mineral deposits, as they contain pyrite, marcasite, sphalerite, galena and baryte; many deposits also contain high concentrations of pyrrhotite and celestite.

Bacteriogenic limestones created during caprock formation are an important ore host in this style of deposit. However, diapir and allochthon caprocks are no longer considered to reflect an exclusively meteoric setting, and so mineralisation models are still evolving for this style of deposit. The popular consensus of caprock genesis is shifting more to a sub-sea floor mode for most caprocks. All that is required to form the anhydrite portion of a caprock is that the top of the diapiric salt stem or sheet be bathed in a solution that is undersaturated with respect to halite. To form the calcite portion from this anhydrite/gypsum precursor requires the presence of organics/hydrocarbons and of sulfate-reducing bacteria in the region of the calcium sulfate cap. Such a situation exists sub-sea floor, as well as in zones of continental meteoric circulation. Active marine calcite caprock is forming today at deep sea-floor sites atop shallow salt diapirs and allochthonous salt sheets in the present day Gulf of Mexico (Kennicutt *et al.* 1985; Roberts *et al.* 1990). These sites are coincident with petroleum/methane seeps, so that the calcite cap, including that in entrained mollusc shells, has isotopic signatures indicating a crude petroleum source. Mineralising brines in such areas can be 'exhaled' on to the sea floor to form brine pools in depressions adjacent to the same salt seeps. Given that methane and brine are seeping today into offshore sediments in active salt structure provinces, and that sulfide smokers accompany some of these seeps (Martens *et al.* 1991), it is likely that diapir-hosted sulfides are also forming today beneath the brine pools adjacent to these seeps (see later).

Pb–Zn sulfides begin forming as soon as an anhydrite caprock carapace encrusts a developing salt structure (Kyle & Posey 1991). This can happen during the earliest phases of salt flow and continue, perhaps episodically, as long as the structure's crest is bathed in near-surface halite-undersaturated waters and oil- or methane-bearing fluids continue to circulate near the diapir (Figure 9b). Some of the earliest minerals to form in the caprock are sulfides precipitated in equilibrium with anhydrite, where they often form laminar sulfide–anhydrite textures controlled by the morphology of the dissolution interface (Price *et al.* 1983). As crude oil and thermogenic methane migrates up a diapir's margin to encounter anhydrite/gypsum within a low temperature environment (~80°C), biogenic calcite forms as a by-product of bacterial sulfate reduction. Sulfides, baryte and celestite can form at the same time or post-date the calcite. Gypsum caprock continues to form after anhydrite, and calcite caprock interfaces are well established, typically through the ongoing infiltration of undersaturated near-surface waters that ultimately will rehydrate any remaining anhydrite (Werner *et al.* 1988).

Thus, at any particular site in a caprock deposit, iron sulfides typically form early; galena and sphalerite form later; and baryte, celestite and sulfur are generally the last phases to precipitate. Banded or colloform textures consisting of finely crystalline aggregates are the most common textures exhibited by the iron sulfides and sphalerite. These base-metal sulfides occur as inter-anhydrite crystal cements, open-space fills in anhydrite, as carbonate/sulfate replacements, and as open-space (vug/cavity) fills. Most of the anhydrite-hosted mineralisation formed during anhydrite caprock accumulation, whereas most of the sulfides hosted in biogenic calcite formed prior to or during calcite precipitation (Kyle & Price 1986).

In general, an anhydrite caprock accretes or thickens by growth along its underbelly by a process of underplating. As diapiric salt dissolves from the uppermost portions of the underlying halite stem/sheet, it leaves behind the entrained anhydrite as a residue (Figure 9b). Calcitic caprock also forms first at its bottom, but it does so by the progressive bacteriogenic replacement of the underlying calcium sulfate (Light & Posey 1992). Metal sulfides that precipitate syngenetically within either the anhydrite or the calcite caprocks show isotopic compositions and major element compositions that vary with depth. This range in isotopic values may record chemical changes in upward migrating metal-bearing brines or changes in local chemical conditions relating to bacteriogenic overprints during sulfide precipitation. The range in metal concentrations most likely reflects changes in brine composition due either to brine mixing or to evolution of brine composition. Episodes when metalliferous brine entered accreting diapir caprocks are recorded as relatively thin bands of sulfide sandwiched between thicker bands of anhydrite. Continued dissolution of salt and underplating of residual anhydrite caused the sulfide bands to be displaced upward relative to the base of the cap, leading to an inverted stratigraphic record of basin dewatering events.

Peri-allochthon-hosted stratiform base-metal laminites

As well as forming in the diapiric caprock, Pb–Zn deposits can be hosted in organic-rich pyritic and sideritic laminites located centripetal to salt sheets or halokinetic breccias, so making them stratiform peridiapiric ore deposits. The highly reduced, organic-rich, nature of laminated peridiapiric sediments means that framboidal pyrite easily forms as a syndepositional precipitate. As this pyrite is buried deeper into the brine/hydrothermal system it is bathed and altered by escaping metalliferous basinal brines. Examples of this brine pool style of mineralisation range from small- to medium-scale Pb–Zn accumulations, such as Bou Grine in North Africa, to world-class sulfide laminites, as are found today beneath the brine lakes on the deep sea floor of the Red Sea.

ALLOCHTHONS AND METALLIFEROUS LAMINITES

As an allochthonous salt sheet lies just beneath the sea floor, it dissolves from its edges inward and releases chloride-rich brine into its surrounds. Any subsalt brine forms a dense chloride-rich plume that then sinks into the underlying sediments and so becomes caught up in subsalt convection cells. As it convects, it mixes with escaping basinal brines whose upward passage is focused along the

dissolving undersides and edges of the salt allochthon, before it finally seeps and vents to the sea floor. For example, brine-issuing vents occur at 1920 m-deep sea floor on top of Green Knoll, which is an isolated salt allochthon rising seaward of the Sigsbee Escarpment in the northern Gulf of Mexico. Vent brines are supplied in part by congruent seawater dissolution of the underlying Louann salt, and in part by salt-focused hydrocarbon-rich basinal waters escaping from deeper in the sediment column (Aharon *et al.* 1992). The venting brines are seven times saltier than ambient seawater and the geometry of their subsurface passage to the sea floor largely reflects breaks in the continuity of allochthonous salt sheets that underlie much of the continental slope of the Gulf of Mexico (Thrasher *et al.* 1996).

Locally, the anoxic brines will pond on the deep sea floor wherever vented brines can seep into closed sea-floor depressions. There must be three-way closure in the sea-floor depression for a brine lake to form. The lows form by subsidence atop dissolving shallow allochthonous salt sheets or atop areas of salt withdrawal where the underlying salt is flowing into adjacent growing salt structures (allochthons and diapirs). The redox interface in such sea-floor lakes is located at the halocline and so may be located some metres or tens of metres above the sea-floor. For example, the Orca Basin in the Gulf of Mexico is a closed intra-slope depression at a depth of 2400 m, some 600 m below the surrounding sea floor (Figure 10a). Its bottom is filled by a 200 m-column of highly saline (259‰) anoxic brine that is more than a degree warmer than the overlying seawater

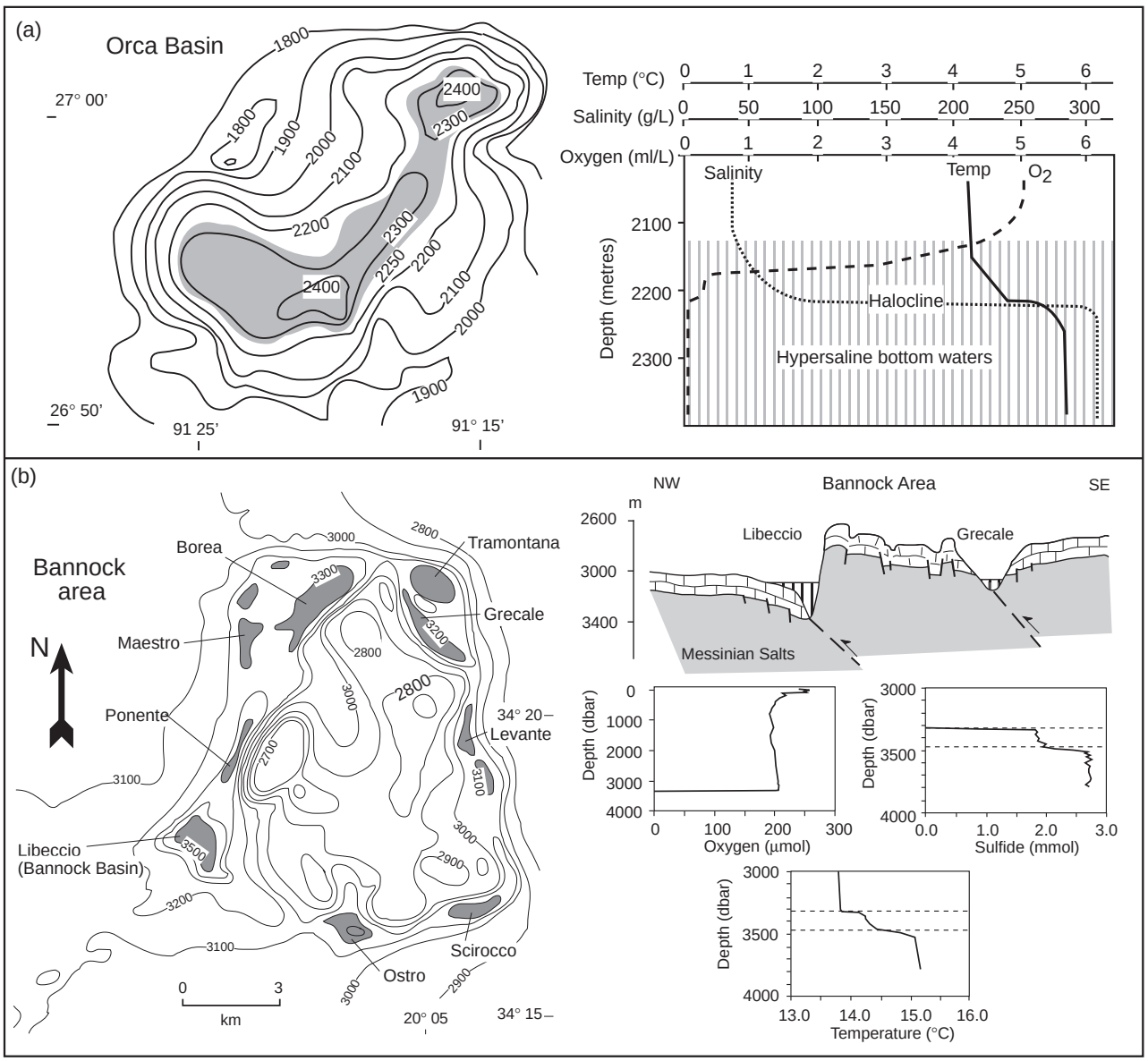

Figure 10 Sea-floor brine lakes. (a) Orca Basin, northern Gulf of Mexico showing location and bathymetric profile (metres below sea level) as well as temperature, salinity and oxygen profile through waters of the brine lake. Grey area shows extent of sea-floor brine lake underlain by organic laminites (after Williams & Lerche 1987). (b) Brine lakes on the deep sea floor of the Mediterranean showing bathymetry (lakes in grey) as well as cross-section and oxygen, sulfide and temperature profiles (after Camerlenghi 1990; Bregant *et al.* 1990; Warren 1999).

column (Figure 10a). The pool is stable and has undergone no discernible change since it was first discovered in the 1970s. It is a closed dissolution depression fed by brines seeping from a nearby subsurface salt allochthon (Addy & Behrens 1980). A large portion of the particulate matter settling into the basin is trapped at the salinity interface between the two water bodies. Trefry *et al.* (1984) noted that the particulate content was 20–60 μg/L above 2100 m and 200–400 μg/L in the brine column below 2250 m. In the transition zone, the particulate content was up to 880 μg/L and contained up to 60% organic matter.

A core from the bottom of the Orca brine lake captures laminated black organic-enriched pyritic mud from the sea floor to 485 cm depth and entrains three intralaminite turbidite beds of grey mud with a total thickness of 70 cm (Addy & Behrens 1980). This is underlain by grey mud from 485 cm to the bottom of the core at 1079 cm. The laminated black mud was deposited in a highly anoxic saline environment, while grey mud deposition took place in a more oxic setting. The major black–grey boundary at 485 cm depth has been radiocarbon dated at 7900 ± 170 a and represents the time when escaping brine began to pond in the Orca Basin depression. Within the dark anoxic laminates of the Orca Basin there are occasional millimetre- to centimetre-thick red layers where the iron minerals are dominated by hematite and other iron hydroxides and not by pyrite. These layers represent episodes of enhanced mixing and oxygenation across the normally stable halocline and indicate the short-term destruction of bottom brine stratification.

Brine pools do not just form by allochthon solution on the floors of rifts and passive margins, they also form in the compressive terrain of the central and eastern Mediterranean where sheets of Miocene evaporites have been folded and thrust to shallow depths below the deep sea floor. The consequent dissolution of the near-surface salts is creating saline brine pools. Two of the better studied marine regions with hypersaline deep bottom waters are the Tyro Basin and Bannock area (Camerlenghi 1990). In the latter area, the various brine-filled depressions or subbasins create a closed outer moat around a central sea-floor mound that is 10 km across (Figure 10b). As in the Orca Basin, the organic content of these brine-pool bottom sediments is much higher than is found in typical deep sea-floor sediment (>1–3% TOC).

The anoxic hypersaline brines of the Tyro and Bannock Basins are among the most sulfidic bodies of water in the marine environment, with H_2S concentrations consistently greater than 2–3 mmol (Figure 10b) (Henneke *et al.* 1997). In contrast, there is little to no H_2S in the anoxic bottom brine of the Orca Basin. There the iron concentration is 2 ppm, a value more than 1000 times higher than in the overlying Gulf of Mexico seawater. Such high levels of reducible iron in the Orca Basin are thought to explain the lack of H_2S in the bottom brine and a preponderance of framboidal pyrite in the bottom sediments (Sheu 1987). Both the Orca Basin and the brine pools on the floor of the Mediterranean show sulfate levels that are more than twice that of the overlying seawater.

Pyritic sulfur is the main phase of inorganic reduced sulfur in the Tyro and Bannock Basins, where it makes up 50–80% of the total sulfur pool. It is also present at the same levels in cores from the two basins, i.e. around 250 μmol/g dry weight (Henneke *et al.* 1997). Humic sulfur accounts for 17–28% of the total sulfur pool in the Tyro Basin and for 10–43% in the Bannock Basin. Sulfur-isotope data show negative $\delta^{34}S$ values for both pyritic sulfur, with $\delta^{34}S = -19$ to $-39‰$; and for humic sulfur, with $\delta^{34}S = -15$ to $-30‰$; indicating that both pyritic and humic sulfur originated from microbially produced H_2S within the brine column.

Usually, the density of the bottom brine in the Bannock region is high enough to support finely dispersed organic debris, allowing substantial bacterial mats to float at the seawater–brine interface (halocline) and form suspended deep mid-water bacterial mats (Erba 1991). While the organics float on the oxic side of the halocline, they are subject to oxidation and biodegradation. Owing to the high density of the bottom brines, moving this floating organic material to the floor of density-stratified brine pools appears at first to be a difficult proposition. Yet, organic contents in the anoxic bottom muds beneath these pools are as high as 4–5% organic carbon. The propensity for organics to remain suspended at the halocline is overcome when mineral crystals, including pyrite, precipitate at the interface by diffusive brine mixing in combination with bacterial sulfate reduction. Newly formed crystals attach to organic matter floating at the halocline to create a combined density that carries the suspended pellicular organics to the pool floor. In such a brine-pool scenario, the redox front that fixes pyritic sulfur occurs at the halocline, and not at its more typical marine position located at or just below the sediment–seawater interface.

Organic debris then accumulates as preserved pellicle layers within the pyritic bottom muds (laminites). Pellicular debris is also carried to the bottom during the emplacement of turbidites when the halocline is disturbed by turbid overflow (Erba 1991). Hence, pellicular layers are typically aligned parallel to lamination, or are folded parallel to the sandy bases of the turbidite flows, or line up parallel to deformed layers within slumped sediment layers. Individual pellicle layers are 0.5–3 mm thick and dark greenish-grey in colour.

If the evaporite indicators in ancient counterparts of pyritic laminites that form within brine pool/seep systems are not recognised, then once the associated allochthonous salt sheets have dissolved or moved on, an evaporitic association for the organic-rich pyritic brine-pool sediments will become an enigma. Any remaining organic constituents are made up primarily of marine plankton, a benthic marine biota and bacteria from a normal marine setting. Sediments above and below the pyritic pellicular laminites are made up of normal marine deep-water deposits. There will be little geochemical evidence to show these organic-rich pyritic sediments were preserved in a hypersaline deep marine environment. Evidence of the significance of evaporites in creating such a sequence will only come from sedimentological and structural analysis of core or outcrop, and the recognition of halokinetic breccias, salt welds, chemosynthetic biostromes and marine-cemented hardgrounds within a deeper water marine sediment matrix.

Recognition of similar bottom brine systems is even more enigmatic in the Proterozoic, where elevated levels of

methane and CO_2 were the norm for the world's oceans (Grotzinger 1995; Grotzinger & Knoll 1995). In such systems, widespread fibrous calcite and aragonite cementstones/hardgrounds characterised the typical shallow tropical carbonate sea floors as well as the margins of much more localised brine seeps. Unlike today, the Proterozoic sea floor was dominated by splayed acicular cementstones that built decimetre- to metre-thick beds separated by shallow-marine grainstones and rudstones. Such cementstone hardgrounds are widespread in outcropping carbonates of the Proterozoic basins of northern Australia, but have been misconstrued by some previous workers as evaporite indicators (e.g. Coxco structures and sideritic marbles, supposedly after gypsum, in the McArthur Group of the McArthur Basin: see Warren 1999 chapter 9).

Ancient peri-allochthon metalliferous laminite, Bou Grine Pb–Zn, North Africa

The Bou Grine Pb–Zn deposit is situated at the edge of the Lorbeus diapir in the Domes region of the southern Tunisian Atlas (Rouvier *et al.* 1985; Charef & Sheppard 1987, 1991; Orgeval 1991, 1994; Bechtel *et al.* 1996, 1998). Pb–Zn (Ba, Sr, F) mineralisation in the Domes area occurs mainly in Cretaceous cover rocks near the edges of the Triassic diapirs. There are four main mineralisation types: (i) lenticular Pb–Zn (Ba–Sr) Fe bodies in the zone of transition from the Triassic to the Cretaceous host sediment (caprocks); (ii) stratiform Pb–Zn mineralisation in calcareous laminites, which are also rich in organic matter (e.g. Bahloul Formation); (iii) Pb–Zn–Ba–F and Fe–Pb deposits, with features similar to Mississippi Valley-type deposits, in the Aptian reef formations that formed atop sea-floor highs created by salt allochthons; and (iv) vein-type deposits.

Bou Grine mineralisation belongs mostly to the first and second groupings. The Bou Grine deposit differs from subeconomic caprock sulfides in the Gulf of Mexico in that much of the Pb–Zn resides not in diapir cap rock but in the organic-rich limestone laminites of the Bahloul Formation, which were deposited in sea-floor brine lakes adjacent to the diapir. As well, a semi-massive orebody (hangingwall orebody) cuts the Cretaceous series in the second megasequence in the Cenomanian–Turonian Bahloul Formation at Bou Grine. The geologic reserves, with a cutoff value of 4% Pb+Zn, are currently estimated at 7.3 Mt of ore at 2.4% Pb and 9.7% Zn, equivalent to 880 000 t of metal.

The early nature of mineralisation at Bou Grine is reflected in (Bechtel *et al.* 1996): (i) convoluted mineralised laminar beds deformed by intraformational slip, with flow structures; (ii) compaction structures around rigid cores of pyrite nodules and galena crystals; and (iii) deformed infilled fissures. Sphalerite developed as: (i) early regularly disseminated microsphalerite crystals in a slightly compacted sediment; (ii) almost simultaneous concentrations along sedimentary structures, textures and discontinuities; (iii) later concentrations and deformations of the mineralisation due to compaction and subsequent fracturing; and (iv) diagenetic remobilised cements that were either passive infills or provoked by circulation of mineralising fluids.

Laminites of the Bou Grine region also show high total organic carbon contents (4–5% TOC), low organic maturity (T_{max} = 423°C) and a marine (Type II) phytoplankton origin (Bechtel *et al.* 1996). Hydrocarbon enrichment at particular levels suggests possible former hydrocarbon reservoirs in some of the sediments adjacent to the diapirs. Montacer *et al.* (1988) showed that sulfate reduction in the laminite facies was bacterially mediated with evolution of the organic matter probably occurring by *in situ* maturation of the laminite source rock. Their isotope studies support the notion of a close relationship between the initial metal stock and the sedimentological/diagenetic setting. Sulfur isotopes also indicate development of mineralisation in a closed sulfur system. Along with Sr and Pb isotopes, they also show that the deposit, and its aureole, formed under the influence of an organic-rich diagenetic palaeocirculation, with Pb derived from a single source.

The deposit's locality and host-rock geometry is controlled by a feedback between salt flow and the synkinematic movement of the sea floor (Figure 9c). Thus halokinesis and the associated allochthons control: (i) local deposition of conglomerates and breccias adjacent to the highs atop the growing salt allochthons; (ii) local deposition of organic-rich pyritic laminites in areas of brine ponding on deepened sea floor; (iii) tilting of panels of sediments by listric faults activated by the emplacement of allochthons and diapirs; and (iv) overlapping of sedimentary bodies by shoal/shelf progradation or truncation. Halokinesis also led to marked thickness variations of the various facies across the regions by the repetitious pulsation of the active diapir and its ongoing dissolution.

The Bou Grine region, from its beginnings, was a submarine slope at the edge of a structural high. Other than around a few local diapirs and salt allochthons, this area never seemed to have shoaled sufficiently for a true shallow-water carbonate platform to develop. The organic-rich sediments may well have accumulated in this region only in the deeper areas of rim synclines about the active diapirs and salt sheets, hence the localisation of the mineralisation to laminites in the peridiapiric areas. These organic-rich anoxic depressions probably also acted as early sinks for metal concentrations.

Red Sea metalliferous laminites, a world-class peri-allochthon base-metal deposit

In contrast to the relatively small-scale peridiapiric mineralised laminites and breccias in the Bou Grine deposit, the brine-fed deeps on the floor of the Red Sea contain volumes of metal sulfides that rival ancient ore bodies. The southwest portion of the Atlantis II Deep contains 150–200 Mt of unconsolidated mud averaging 5–6 wt% Zn and 0.8 wt% Cu on a dry salt-free basis. These tonnages rival some world-class sediment-hosted base-metal deposits and represent the only known deposit of Fe, Mn, Zn, Cu, Ag and Au of economic proportions currently forming on the sea bottom (Shanks 1983; Backer & Lange 1987). The Red Sea is a young intracratonic basin on a region of the sea floor that is currently transitional from continental to oceanic rifting. Economically, the most important brine pool is in the Atlantis II Deep; other smaller deeps with metalliferous muds include Commission Plain, Hatiba, Thetis, Nereus, Vema, Gypsum, Kebrit and Shaban Deeps.

All these brine-filled deeps are located in depressions along the spreading axis in the region of the median valley. Most of these axial troughs and deeps are also located where transverse faults, inferred either from bathymetric data or from continuation of continental fracture lines, cross the median rift valley in regions that are also characterised by nearby allochthonous Miocene salt (Figure 11a).

Three conditions favour the formation of the brine-filled deeps in the region (Blum & Puchelt 1991): (i) the Red Sea is a narrow depression only 200 km wide, with water circulation to the south limited by a shallow subsea sill near the connection with the Indian Ocean; (ii) the slow rate of clastic or pelagic accretion along the axial part of the rift allows transverse faults to influence the topography of the sea floor; and (iii) nearby dissolving halokinetic salt contributes huge volumes of hydrothermal and basinal brine to an irregular bottom topography it helped create. Many deeps are filled by permanently stagnant brine pools derived either directly from the dissolution of shallow evaporites or overspill from adjacent brine pools. Other deeps, filled or partly filled by episodic hydrothermal brine seeps, may have been intermittently affected by hydrothermal convection in the bottom brine layer.

The Atlantis II Deep, the most economically interesting deep, is roughly elliptical in shape, 14 km long by 5 km wide, and is located in the most geothermally active part of the central Red Sea (Figure 11a). The bottom of the brine pool is 2200 m below sea-level and is flanked on all sides by thick sequences of mobile Miocene evaporites and clastics. Through subsurface dissolution and convective flushing, these Miocene evaporites supply ions to the sea floor and to high-salinity brines caught up in hydrothermal flow cells beneath the salt units. Hot hybrid brines ultimately discharge onto the floor of the deep and settle into the main depression to form a two-layered brine pool some 200 m thick and underlain by hypersaline metalliferous muds (Figure 11b).

The deep was first discovered in 1966. It contains about 5 km^3 of brine, stratified into distinct dense and convective layers of differing temperature and chlorinity. The lower brine body has an area of 1.8 km^2 and is about 150 m thick over a sea bottom as deep as 2040 m (Figures 11b). In 1977 the bottom brine had a temperature of 61.5°C, a chlorinity of 156‰, and contained no free oxygen. The overlying 50 m-thick brine layer of the Transition Zone was at 50°C with an 82‰ chlorinity. This partially oxygenated upper brine was a transitional zone of mixing between the lower brine and overlying normal seawater. Since then there has been a substantial increase in temperature of the brines (Anschutz & Blanc 1995, 1996; Hartmann *et al*. 1998). By 1995 the temperature in the bottom brine of the southwest basin was 71.7°C. The structure of the lower transition zone, between about 1990 m water depth and highly saline bottom brine, has also changed significantly; it now contains two convective layers with nearly constant temperatures (61° and 55°C, respectively). What is most significant is the long-term stability of the lower brine and its isolation from the overlying normal seawater. For the last 26 years, almost all additional heat and salt supplied to the deep was confined to the depression and caused an increase in temperature; very little heat was dispersed into the overlying seawater (Anschutz & Blanc 1996). The rate of heat input to the deep was constant during this period, and amounted to 0.54×10^9 W. The salt input was also constant, and equalled 250–350 kg/s. The effect of this long-term brine pool stability over millennia has been the accumulation of some rather unusual sulfide-rich saline sediments.

In the last 28 000 years, some 10–30 m of the oxidic–silicatic–sulfidic laminites, along with hydrothermal anhydrite, have accumulated beneath the Atlantis brine pond and above the basaltic basement (Figure 11c) (Shanks & Bischoff 1980; Pottorf & Barnes 1983; Anschutz & Blanc 1995). Metalliferous sediments beneath the floor of the deep are composed of stacked delicately-banded mudstones with bright colours of red, yellow, green, purple, black or white indicating varying levels of oxidised or reduced iron and manganese. They are anhydritic and very fine grained, with 50–80% of the sediment less than 2 μm in size. Intercrystalline pore brines constitute up to 95 wt% of the muds, with measured pore salinities as much as 26 wt% (Pottorf & Barnes 1983). The sulfide-rich layers are a metre to several metres thick and form laterally continuous beds that are several kilometres across. Sulfides are dominated by very fine-grained pyrrhotite, cubic cubanite, chalcopyrite, sphalerite and pyrite, and are interlayered with iron-rich phyllosilicates (Zierenberg & Shanks 1983). Sulfur-isotope compositions and carbon–sulfur relations indicate that some of these sulfide layers have a hydrothermal component, whereas others were formed by bacterial sulfate reduction. Ongoing brine activity began in the western part of the deep some 23 000 years ago with deposition of a lower and upper sulfide zone, and an amorphous silicate zone (Figure 11c).

Hydrothermal anhydrite in the Atlantis II sediments occurs both as at-surface nodular hydrothermal beds around areas where hot fluid discharges onto the sea floor and as vein fills beneath the sea floor (Degens & Ross 1969; Pottorf & Barnes 1983; Ramboz & Danis 1990; Monnin & Ramboz 1996). White nodular to massive anhydrite beds in the western basin are up to 20 cm thick and composed of 20–50 μm plates and laths of anhydrite, typically interlayered with sulfide and Fe-montmorillonite beds. The central portion of individual anhydrite crystals in these beds can be composed of marcasite. The lowermost bedded unit in the southwest basin contains much more nodular anhydrite, along with fragments of basalt toward its base. Its 4 m+ anhydritic stratigraphy is not unlike that of nodular anhydrite that hosts sekko oko ore in a Kuroko deposit, except that the underlying volcanics are basaltic rather than felsic (Warren 1999 chapter 9).

The anhydrite-filled veins that cross-cut the laminites act as conduits by which hot, saline hydrothermal brines vent onto the floor of the deep. Authigenic talc and smectite dominate in deeper, hotter vein fills, while shallower veins are rich in anhydrite cement (Zierenberg & Shanks 1983). The vertical zoning of vein-mineral fill is related to cooling of the same ascending hydrothermal fluids, with stable isotope ratios in the various vein minerals indicating precipitation temperatures up to 300°C. Because of anhydrite's retrograde solubility, it can form by a process as simple as heating circulating seawater to temperatures in excess of 150°C. Pottorf and Barnes (1983) concluded that the bedded anhydrite of the Atlantis II Deep, like the vein

fill, is a hydrothermal precipitate. Based on marcasite inclusions in the anhydrite units, it precipitated at temperatures down to 160°C or less. At some temperature between 60 and 160°C, probably close to 100–120°C, the fluid became undersaturated and hydrothermal anhydrite precipitation ceased. Thus, anhydrite distribution in the Atlantis II Deep is related to the solution mixing and thermal anomalies associated with hydrothermal circulation.

In summary, the Red Sea mode of mineralisation requires stable stagnant brine pools in sea-floor depressions along the medial ridge of an active rift in close association with adjacent thick dissolving halokinetic evaporites. The presence of a dissolving salt aquiclude above sea-floor basalt focuses reflux-driven hydrothermal fluids into the outflow zones about the edges of the stable brine pools. Hot metalliferous brines focused by salt allochthons and escaping into the lower convective layers of these pools become widely dispersed across the extent of the deep-water brine pool. During active venting of metalliferous brines, the long-term brine pond facilitates stable anoxia at the sea bottom, as well as intra-brine-pool convection and the dispersal of metalliferous brine away from the immediate vent area. Diffusive mixing at the halocline over the brine pool precipitated metal sulfides, mostly as pyrite framboids that then sank to the bottom carrying with them dispersed organic water. Thus, a stable bottom brine pool increases the area of prepared ground for any subsequent Fe, Pb, Zn and Cu emplacement. The leaching of adjacent thick halite units not only enhances the permanency of the brine pool, it also raises the metal-carrying capacity of hydrothermal brines and increases the reaction rate of any saline fluids flushing metals from the basaltic basement and suitable first-cycle sediments.

Peri-allochthon/peridiapiric Pb-Zn model: the deposit scale

A model for peridiapiric Pb–Zn accumulations, based in part on the sulfide paragenesis in the Gulf Coast and in the North African deposits as well as modern sea-floor brine pools including the Red Sea laminites, is presented as Figure 9c. Once near the sea floor, a flowing and dissolving salt allochthon or diapir acts as a focus for migrating metalliferous fluids as: (i) sediment slippage and faulting driven by salt flow and dissolution about a diapir or

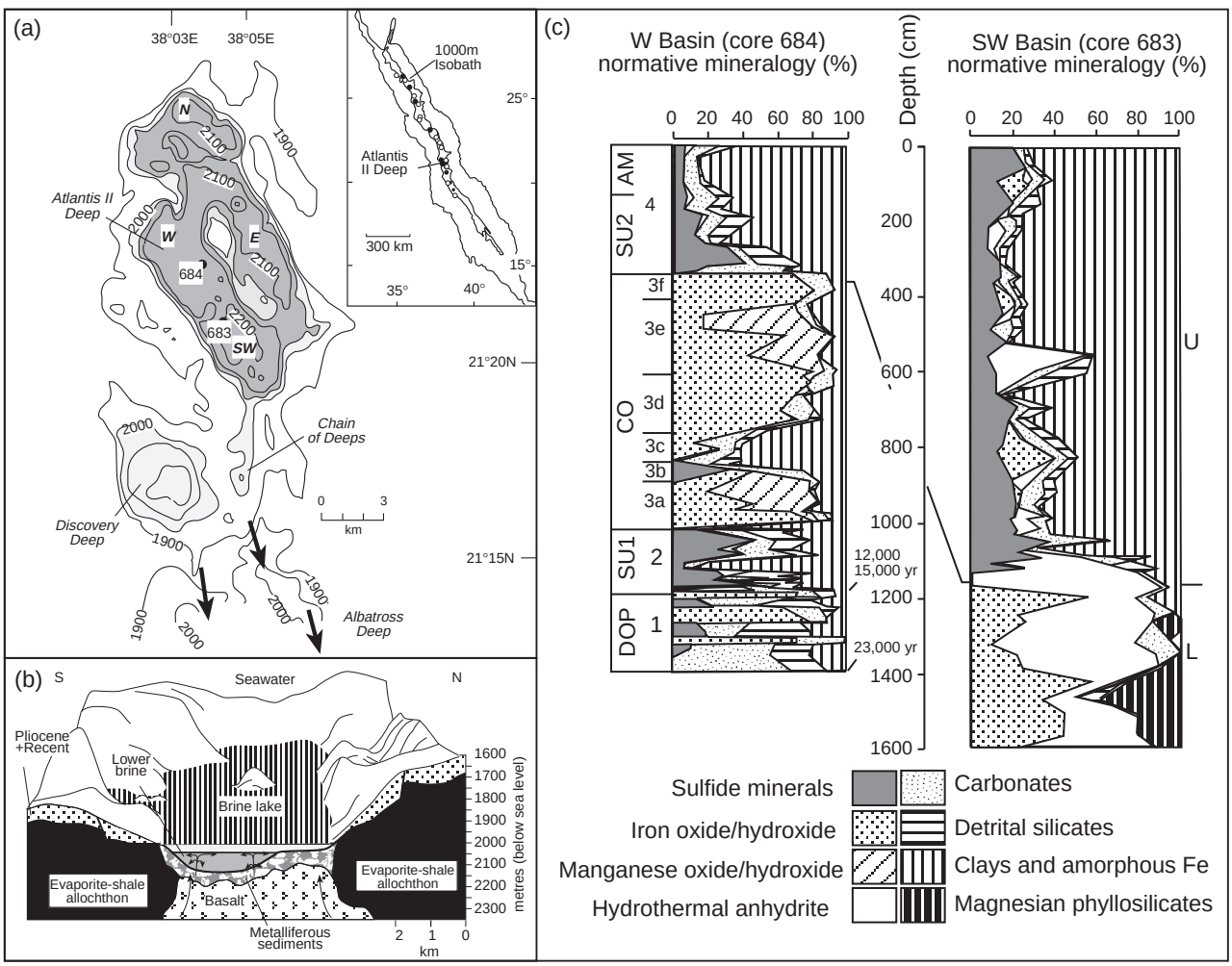

Figure 11 Atlantis II Deep, Red Sea. (a) Location and bathymetry of Atlantis II Deep in the axial trough of the Red Sea. Contours in metres, grey shaded areas show extent of brine lakes (after Anschutz & Blanc 1995; Blum & Puchelt 1991). Open circles in inset map show various brine lakes, closed circles show position of metalliferous brine lakes; all lie beneath waters that are more than 1000 m deep. (b) Schematic diagram of Atlantis II Deep physiography and circulation (after Warren 1999 and references therein). (c) Mineralogical content of representative cores through sediments beneath the brine lake (after Anschutz & Blanc 1995).

allochthon edge provide an ongoing easy passage and focus for upwelling Fe-rich basinal fluids; and (ii) hydrocarbon-saturated caprocks and adjacent organic-rich laminites provide favourable anoxic traps for inflowing metalliferous brine.

Sulfide mineralisation in this system begins with the syndepositional, probably bacteriogenic, accumulation of pyrite framboids within an anoxic organic-rich sediment matrix beneath an anaerobic sea-floor brine pool (Figure 9c). The brine exhaling onto a sea-floor depression makes this deposit style an evaporite-associated subset of sedex (sedimentary exhalative) deposits. The brine pool itself is also a result of the venting of these upwelling highly saline waters. As the pyritic organic-rich laminites are buried, they pass into a new diagenetic environment, which is bathed in hotter, deeper haloes of the same Fe-chloride brines that are escaping at the surface of brine seeps and vents. At the same time as the peridiapiric laminites are forming on the floor of deep-sea brine lakes, metal sulfides are also forming in the fractured and brecciated caprock that is growing atop the crest of the adjacent dissolving salt allochthon (Figure 11b). A deeper burial-imposed equilibrium then favours the replacement of the pyrite precursor by other metal sulfides. The relative proportion of Cu *vs* Pb–Zn in these replacements depends on the temperature and brine chemistry of the throughflushing basinal waters. In effect, peridiapiric mineralisation is part of a fluid-cycling system instigated during early diagenesis and continued into deeper burial under a plumbing that is controlled by basinal faults and tectonics that are in turn driven by halokinesis.

As in anoxic brine pools elsewhere in the world (Warren 1999 chapter 9), the reduced sulfur in the shallow pore brines and the bottom brine layer were mostly derived from bacteriogenic reactions using seawater sulfate and entrained organic matter. This created conditions suitable for widespread metal-sulfide precipitation at the halocline, in the brine column, and in brine-saturated sediments beneath areas covered by stable anoxic H_2S-enriched brines. Brine-pool stability (density contrast) prevented widespread dilution via mixing with overlying seawater and so allowed metal sulfides to accumulate across large areas of the brine pool floor and not just near vent localities. Some of the higher temperature hydrothermal basinal brines seeping into these brine pools may have been carrying H_2S at the same time they carried the metals (Barnes 1979). Such simultaneous transport can only occur at higher temperatures where sulfide solubility and chloride complex stability can coexist.

Such deposits form by salt-tectonic focusing of escaping metalliferous basinal brines into local brine-filled anoxic deeps where the subsurface passage of the salt-solution-derived Fe-chloride rich brines that feeds pools is indicated by Fe-carbonate haloes along faults and glide shears (Warren 1999). However, the ferroan carbonate haloes are not deposit or formation specific, and can be found over much wider areas than the immediate region of metalliferous laminites. The accumulation of substantial sulfides, especially pyrite framboids formed in the early stages of sulfide accumulation, requires the presence of anoxic bottom brines in the deeper portions of isolated depressions on the shelf floor. For stable anoxic brine lakes to form on the sea floor requires a completely enclosed depression (this three-way closure requirement has important implications for exploration models).

Allochthon-associated laminite/sedex model: the regional scale

Not all pyritic laminite/sedex deposits are associated with salt allochthons. The following allochthon model can only be applied to shelf and slope basins whose sedex/metalliferous laminite-entraining depopods show abundant evidence of former widespread evaporites. Evidence of syn-laminite salt flowage is typically found in intervals in or below the potential ore horizons. For example, the textural and structural features found in some Proterozoic sedex deposits in northern Australia imply that metalliferous brine escape was perhaps created and focused by dissolving salt allochthons (e.g. laminites of the HYC deposit, portions of the Mt Isa laminites, and perhaps the Century deposits: Warren 1999 chapter 9). Such deposits are typified by: (i) underlying and syndeformational evaporite solution breccias; (ii) ongoing soft-sediment extensional faulting, which breaks up the continuity of individual ore layers; (iii) syndissolutional and syndepositional soft-sediment folds showing poor vergence and axial trends; (iv) framboidal pyritic and organic-rich nature of the ore host sediment; (v) localised syndepositional thickening/deepening of the ore-hosting formation within an otherwise shallower water setting; (vi) ferroan carbonate halo distribution about faults, especially along the intrashelf basin edge; and (vii) syndepositional extensional graben structuring and consequent compression.

Allochthonous salt sheets and diapirs in all salt tectonic realms can act as focusing zones for metalliferous basinal fluids; this happens from initial salt deposition until complete salt dissolution. Complete salt dissolution, which shuts down brine supply, can occur at any time in the diagenetic burial or metamorphic realms. While salt is present: (i) impervious diapir and salt sheet margins provide an ongoing focus for upwelling basinal fluids that typically feed into suprasalt extensional faults; (ii) ongoing salt flow creates large suprasalt structural folds and hydrocarbon/metal traps, such as rollover anticlines, while overlying or adjacent depopods fill with organic-rich laminites; these features always form and grow next to extensional faults or compressional faults created by salt flow; (iii) depending on the lateral extent of an underlying and lubricating salt allochthon, the actively accumulating sediment pile above the salt layer can be undergoing extension in one area while simultaneously undergoing compression in another; and (iv) the organic-rich laminite-filled depopods are covered and flushed by metalliferous brines from the time of their formation through into the burial diagenetic/metamorphic realm, and so are favourable subsurface traps for metals and hydrocarbons.

Sulfide mineralisation in a halokinetic platform or slope can begin in a bottom brine pool by the syndepositional, probably bacteriogenic, precipitation of pyrite framboids in an anoxic organic-rich laminite matrix. It can continue into much greater burial depths as ongoing focused hydrothermal alteration processes overprint early formed sulfides by the passage of increasingly hotter chloride-rich

waters along the millimetre-scale permeable intervals in the laminites. Throughout, the feeder faults are kept active and permeable by ongoing collapse and extension generated by the deforming and dissolving salt unit that underlies the sulfide accumulation. This salt-flow-induced jiggling of sediments above the salt bed helps trigger the numerous soft-sediment faults and slumps that are so obvious in the ore-hosting laminites. As these metalliferous laminites are buried they pass into shallow sub-sea-floor diagenetic environments that are part of a hotter, deeper feeder zone for the same Fe-chloride brines that are escaping at the sea-floor brine seeps about the edge of the brine lake. A burial-imposed equilibrium favours the replacement of the pyrite precursor by Pb–Zn sulfides. In effect, mineralisation in salt-solution-controlled basins is a fluid-cycling system, instigated by early diagenetic facies controls, and continued into burial diagenetic situations. The plumbing is largely controlled by basinal faults, which in turn are generated by halokinesis and salt dissolution.

What distinguishes the hydrothermal salts and widespread metalliferous laminites in the peri-allochthonous Atlantis II Deep from the somewhat smaller Bou Grine styles of mineralisation, is that the hot metalliferous brines now found on the Red Sea sea floor achieved their elevated salinities and acidic, saline chemistries by hybrid hydrothermal circulation of seawater, both through the sea-floor basalts and through the adjacent redbeds. Substantial areas of both lithologies are covered and sealed by the dissolving and flowing salt allochthon (Figures 9, 12). That is, salt-solution-enhanced sub-allochthon circulation first occurs in synrift time, when the nearby active igneous mass has maximised thermal- and density-driven circulation of both seawater and hypersaline brines. Active density- and thermal-driven circulation enhances the potential supply of metals to the hydrothermal system and ultimately to the brine lakes on the deep sea floor. Heat to drive this circulation probably comes from the hot basaltic magmas in the slowly spreading axial zone, while most of the chloride and fluid focusing was contributed by hydrothermally circulating seawater and nearby dissolving salt allochthons. Thus a seawater/brine flushing of newly formed basalts, as well as of sub-salt sediments, both contribute metal to the brine pool. This is clearly seen in studies of lead isotopes in the brine-pool laminites, which indicate that a substantial portion of the lead came from the Miocene evaporitic strata and not from the basalts (Dupre *et al.* 1988).

Not only can peri-allochthon sedex deposits form in such a system, but subsalt 'MVT'-style passive-margin deposits, such as Gays River and Jubilee, and Kupferschiefer-style Cu deposits, can be forming simultaneously below the salt allochthon/bed in zones of appropriately focused brine flow (Figures 4b, 7b, 12). In these deeper burial settings, the metal sulfides are especially likely to precipitate in areas where rising basinal brines encounter sulfate evaporites, which then act as reductants (H_2S), or where the focusing salt bed has a geometry that traps hydrocarbons.

The effect of the salt blanket (allochthon or mother salt bed) is to act as a focus to upwelling basinal and hydrothermal fluids as well as supplying dense chloride-rich brine to the underlying convective system. The lateral extent of the salt sheet controls the volume of fluid that is focused along its edge. Hence, beneath those salt layers that are not allochthon tiers inserted higher in the post-rift stratigraphy, the area draining into the focused outflow zone can be huge and the resulting deposits world class (e.g. Kupferschiefer, Lubin). If the area drained is smaller, as it is in some of the tiered allochthons of Tunisia and the Gulf Coast, then the volume of emplaced peri-allochthon metals will likewise be smaller. The lithology beneath the salt blanket also exerts important controls on the make-up of the precipitated sulfides. If the salt unit sits above or adjacent to a redbed sequence or a volcanic pile the resulting metals precipitates will tend to be Cu-rich (as is the case in Atlantis II, Dzhezkazgan and the Kupferschiefer ores). If, on the other hand, the underlying brines are circulating within siliciclastics or carbonates the resulting metal sulfides will be rich in Pb and Zn (Bou Grine and Gulf Coast).

DEFINING CRITERIA

If a dissolving salt bed or allochthon is creating an evaporite-associated sedex/laminite deposit, then the following features should be present in the rock matrix (Figure 12) (the list passes from the general to the specific).

(1) General evidence for former salt beds in particular horizons and tectonic settings within the stratigraphy. Thick salt beds tend to accumulate at times of basin-wide restriction associated either with early continental rifting or with continent–continent collision and transfer/tear faults. The salt beds in a rift setting typically overlie and seal thick sequences of immature synrift sediments composed of volcaniclastics, redbeds and organic-rich shales. All these lithologies are likely to act as metal sources during brine reflux-induced metal flushing. In Precambrian sediments, where the former salt unit has long since gone, the solution breccias of the mother salt bed (primary weld) tend to occur above or immediately below major sequence boundaries. Secondary salt welds or tiers can occur higher in the stratigraphy and define intervals where the former salt unit was encased in normal marine sediments. Such intervals are typically much more difficult to identify once the salt has moved on or dissolved.

(2) Structural styles and faulting patterns that indicate gravity gliding and possible raft tectonics occur above the salt bed/breccia (a major décollement). Many depopod-defining faults sole into major evaporite layers/breccias.

(3) Abundant evidence for fault-fed ferroan carbonate replacement haloes (feeder haloes may also entrain minor metal sulfides and baryte).

(4) Evidence of these large faults intersecting a pyritic/sideritic interval and so lying adjacent to a possible brine pool or structurally closed deposit where the precipitating redox front was located.

(5) Evidence for a salt-solution breccia/former salt bed beneath deeper water pyritic deposits. If the salt bed was an allochthon, then the primary salt/fault welds and the original salt bed, may lie much deeper in the stratigraphy. In this case, salt allochthons may be encased in normal marine sediments, which contain no evidence of an evaporite depositional setting. This is an extremely important determination, and the explorationist must be able to separate tectonic from sedimentary and salt-solution breccias,

even when the sandwiching lithologies are normal marine. Recognising indicators of vanished evaporites is very important.

Feeder faults to sedex systems may be reactivated during any subsequent time of extension or compression and basin inversion. Time frames for reactivation can range from less than ten to hundreds of million years. In such a scenario, the feeder faults may evolve into reverse faults, and associated halokinetic solution breccias can become preferred conduits for cupriferous hydrothermal waters that are squeezed from the basin by compressional forces. Alternatively, as the solution-breccia beds are more deeply buried they pass into a temperature range suitable for the emplacement of copper from hotter basinal brines. Their higher permeability means they may become preferential conduits for cupriferous basinal brines. Such reactivation scenarios are possible explanations for the 100 million year plus gap at Mt Isa between the formation of the Pb–Zn laminites and the copper mineralisation hosted in a dolomitised metabreccia that still retains evidence of evaporite pseudomorphs.

A specific exploration paradigm for evaporite-associated sedex deposits in a basin of interest cannot be generalised from a single halokinetic model. Salt can 'flow and go' at all times from early burial through to amphibolite facies, and can create multiple tiers of deformation and regional-scale faults as it does so. Thus, it is extremely important to define the style of breccia and its structural paragenesis, so that it then can be assimilated into a metal-exploration model. Features such as evaporite dissolution breccias or stratabound pseudomorph horizons should be sought, even during the initial reconnaissance stages. As we have seen throughout this series of reviews, evaporite beds are important foci for fluid flow and in many cases for mineral precipitation. In regions where such prospective strata intersect faults at depths suitable for exploitation, then a more detailed targeting program can come into play.

CONCLUSIONS

Salt acts in various ways to help form Cu and Pb–Zn deposits in the diagenetic realm. Subsurface evaporites are important foci and sources for high-salinity brines; they play a fundamental role in fluid-escape pathways. Thus mineralisation can be subsalt, intrasalt, or suprasalt and the salt body, or its breccia, can be bedded or halokinetic (Table 1).

The diagenetic evaporite – base-metal association includes world-class Cu deposits, such as the Kupferschiefer-style Lubin deposits of Poland and the large accumulations in the Dzhezkazgan region of Kazakhstan. The Lubin deposits are subsalt and occur where long-term dissolution of overlying salt, in conjunction with upwelling

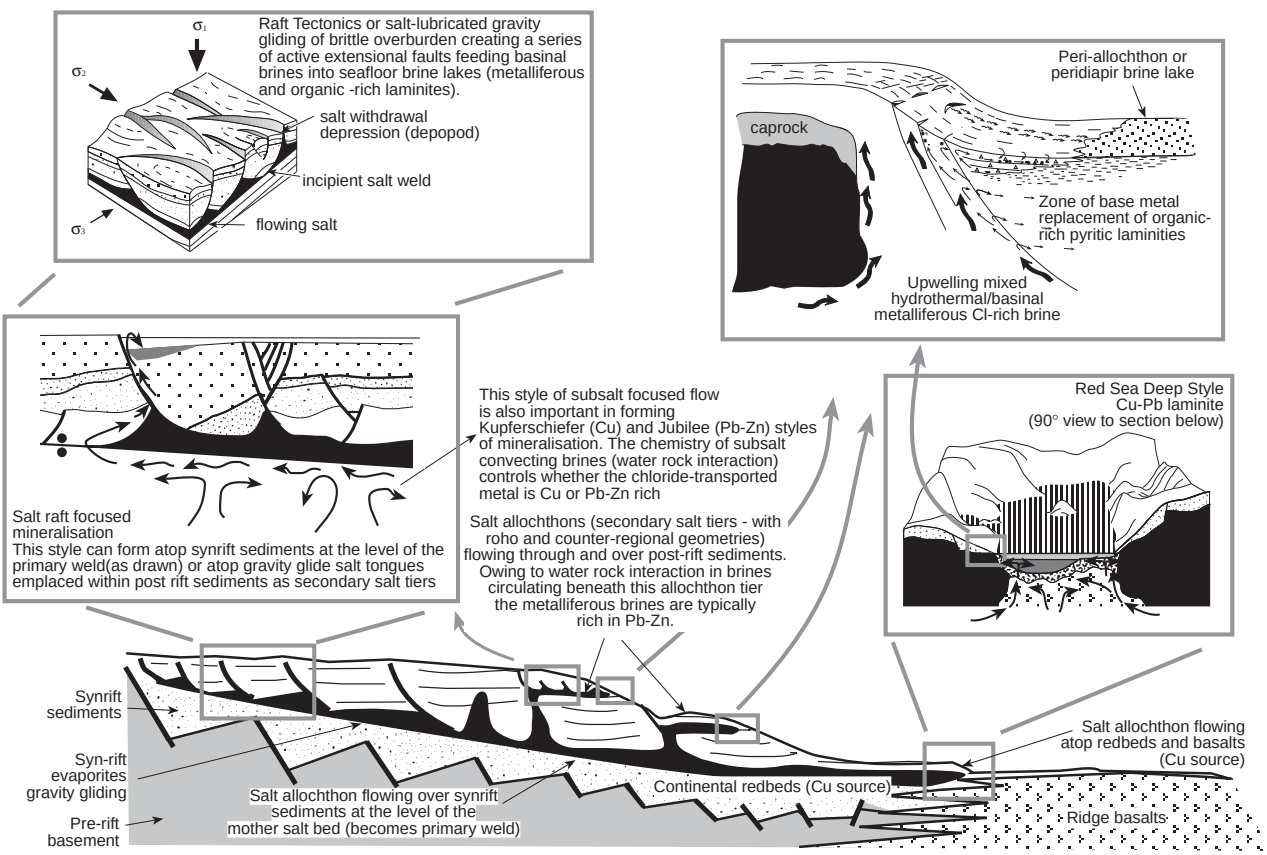

Figure 12 Model of salt-allochthon-controlled base-metal (sedex) accumulation. Note the importance of the subsalt lithologies in controlling the mineralogy of the precipitates. Cu is not easily transported too far from its source beds whereas Pb–Zn can be carried much further. The volume of sediment being leached of its metals beneath the focusing salt unit is controlled by the continuity of the salt bed (published with permission of JK Resources Pty Ltd).

Table 1 Base-metal deposits formed in the diagenetic realm during evaporite diagenesis.

Deposit (age of host)	Reserves (Mt)	Cu (%)	Pb (%)	Zn (%)	Evaporite role	Evaporite association
Bedded stratabound						
Kupferschiefer-style, Lubin, Poland (Permian)	2000	>2	–	–	Subsalt, stratiform with brine focus creating Rote Faule contact and adjacent redox precipitates.	Anhydrite and halite in Zechstein hangingwall and anhydrite in Rotliegende footwall.
Gays River, Nova Scotia (Carboniferous)	2.4	–	8.6	6.3	Subsalt with subsalt focusing of upwelling brine. Local supplier of sulfur via TSR.	Anhydrite both within main ore zone and as cement in disseminated ore.
Creta, Oklahoma, USA (Permian)	1.9	2	–	–	Intrasalt bedded (breccia), adjacent redox precipitates.	Redbed–evaporitic mudflat host with $CaSO_4$ in hangingwall and footwall. Former thick halite beds.
Corocoro, Bolivia (Tertiary)	7	5	–	–	Intrasalt bedded, brine reductant (breccia).	Redbed/greenbed host with gypsum and baryte in veinlets and disseminated nodules.
Redstone River, Canada (Neoproterozoic)	small	2.7	–	–	Intrasalt stratabound with subsalt focusing of upwelling brine.	Algal limestone host with abundant nodular $CaSO_4$.
San Vicente, Peru (Triassic–Jurassic)	12	–	1	12	Intrasalt bedded. Local supplier of sulfur via TSR.	Ore hosted in cryptalgal laminites with pseudomorphs after nodular $CaSO_4$ in barrier-lagoon host.
Cadjebut, Australia (Devonian)	3.8	–	17 (Pb+Zn)		Intrasalt bedded (breccia). Local supplier of sulfur via TSR.	Bedded nodular anhydrite as lateral equivalent to each ore lens with intervening solution breccias.
Allochthon associated						
Atlantis II Deep, Red Sea	150–200	0.8	yes	5–6	Suprasalt allochthon acts as focus to resurging Cu–Zn–Cl brine (salt partially covers ridge basalts).	Dissolving allochthon underbelly supplies Cl-rich metalliferous brine to deep sea-floor brine lake. Hydrothermal anhydrite interbedded with laminites.
Dzhezkazgan, Kazakhstan (Carboniferous)	400	1.5	0.1–1	–	Suprabasalt diapiric, anticlinal focus to brine flow.	Interbedded redbed and greybed host with $CaSO_4$ and halite in underlying salt anticline and lateral equivalents.
Lisbon Valley, Utah, USA (Cretaceous)	small, <0.15	1.4	–	–	Suprasalt allochthon, salt movement creates ore-hosting faults in overburden.	Ore in vein and pore fills adjacent to faults created by halokinesis.
Dongchuan deposits, China (Mesoproterozoic)	10–100	1–1.5	–	–	Suprasalt allochthon or intrasalt breccia. Allochthon acts as focus to resurging metalliferous basinal brine.	Stratabound ore in cryptalgal laminites adjacent to diapiric breccia.
Bou Grine, Tunisia (Cretaceous)	7.3	–	2.4	9.7	Suprasalt laminites. Allochthon acts as focus to resurging metalliferous basinal brine.	Ore in peridiapiric organic-rich pyritic laminites, adjacent to halite of allochthonous diapir sheets.
Gulf Coast, USA (Cretaceous)	not economic	trace	yes	yes	Suprasalt allochthon capstone, brine focus from halokinesis.	Anhydrite caprock undergoing bacteriogenic alteration in association with reservoired hydrocarbons.
Jubilee, Nova Scotia (Carboniferous)	0.9	–	1.4	5.2	Subsalt allochthon (tectonic breccia), stratiform, subsalt focusing of brine.	Interstratified fractured carbonate and anhydrite ore host, created by regional salt-induced gravity slide.

TSR, thermochemical sulfate reduction.

metalliferous basin brines, created a stable redox front, now indicated by the facies of the Rote Faule. The Dzhezkazgan deposits (as well as smaller scale Lisbon Valley-style deposits) are suprasalt halokinetic features and formed where a dissolving halite-dominated salt dome maintained a structural focus to a regional redox interface. Halokinesis and dissolution of the underside of the salt bed also drove the subsalt circulation system whereby metalliferous saline brines convectively leached underlying sediments. In both scenarios, the resulting redox-precipitated sulfides are zoned and arranged in the order Cu, Pb, Zn as one moves away from the zone of salt-solution-supplied brines. This redox zonation can be used as a regional pointer to both mineralisation and to the position of a former salt bed. In the fault-fed suprasalt accumulations the feeder faults were typically created and maintained by the jiggling of brittle overburden blocks atop a moving and dissolving salt unit. A similar mechanism localises many of the caprock replacement haloes seen in the diapiric provinces of the Gulf of Mexico and northern Africa.

Evaporite-associated Pb–Zn deposits, like Cu deposits, can be associated with brine flow associated with both bedded and halokinetic salt units or their residues. Stratabound deposits, such as Gays River and Cadjebut, have formed immediately adjacent to or within the bedded salt body, with the bedded sulfate acting as a sulfur source. In diapiric deposits the Pb–Zn mineralisation can occur both within a caprock or adjacent to the salt structure as replacements of peridiapiric organic-rich pyritic sediments. In the latter case the conditions of bottom anoxia that allowed the preservation of pyrite were created by the presence of brine springs and seeps fed from the dissolution of nearby salt sheets and diapirs. The deposits in the peridiapiric group tend to be widespread, but individual deposits tend to relatively small and most are subeconomic. However, their occurrence indicates an active metal-cycling mechanism in the basin and, given the right association of salt allochthon, tectonics and brine ponding, can form the much less common but world-class replaced laminites. This set of diagenetic brine-focusing mechanisms are active today beneath the floor of the Atlantis II Deep and are thought to have their ancient counterparts in deposits such as Proterozoic McArthur River (HYC) in the McArthur Basin (Warren 1999)

In all these evaporite-associated low-temperature diagenetic ore deposits there are four common factors that can be used to recognise suitably prepared ground and so improve the ability of an exploration model to predict likely sites of ore occurrence within a basin: (i) a dissolving evaporite bed acts either as a supplier of chloride-rich basinal brines capable of leaching metals, or as a supplier of sulfur and organics that can fix metals; (ii) where the dissolving bed is acting as a supplier of chloride-rich brines, there is a suitable nearby source of metals that can be leached by these basinal brines (redbeds, thick shales, volcaniclastics, basalts); (iii) there is a stable redox interface where these metalliferous chloride-rich waters mix with anoxic waters within a pore-fluid environment that is rich in organics and sulfate/sulfide/H_2S; and (iv) there is a salt-induced focusing mechanism that allows for a stable, long-term maintenance of the redox front, e.g. the underbelly of the salt bed (subsalt deposits), a dissolution or halokinetically maintained fault activity, the overburden (suprasalt deposits), a stratabound intrabed evaporite dissolution front (intrasalt deposits).

To put it all in a single sentence: salt beds and salt allochthons are transient features in most sedimentary basins that through their flow and dissolution can dissolve, focus and fix base metals.

REFERENCES

Addy K. S. & Behrens E. W. 1980. Time of accumulation of hypersaline anoxic brine in Orca basin (Gulf of Mexico). *Marine Geology* **37**, 241–252.

Aharon P., Roberts H. H. & Snelling R. 1992. Submarine venting of brines in the deep Gulf of Mexico: observations and geochemistry. *Geology* **20**, 483–486.

Anschutz P. & Blanc G. 1995. Chemical mass balances in metalliferous deposits from the Atlantis II Deep, Red Sea. *Geochimica et Cosmochimica Acta* **59**, 4205–4218.

Anschutz P. & Blanc G. 1996. Heat and salt fluxes in the Atlantis II Deep (Red Sea). *Earth and Planetary Science Letters* **142**, 147–159.

Aref M. A. M. 1998. Biogenic carbonates—are they a criterion for underlying hydrocarbon accumulations—an example from the Gulf of Suez region. *American Association of Petroleum Geologists Bulletin* **82**, 336–352.

Armstrong J. P., Longstaffe F. J. & Hein F. J. 1993. Carbon and oxygen isotope geochemistry of calcite from the Jubilee Zn–Pb deposit, Breton Island. *Canadian Mineralogist* **31**, 755–766.

Arne D. 1996. Thermal setting of the Cadjebut Zn–Pb deposit, Western Australia. *Journal of Geochemical Exploration* **57**, 45–56.

Backer H. & Lange K. 1987. Recent hydrothermal metal accumulation, products and conditions of formation. *In:* Telecki P. G., Dobson M. R., Moore J. R. & von Stackelberg U. eds. *Marine Minerals*, pp. 317–337. Reidel, Dordrecht.

Barnes H. L. 1979. *Geochemistry of Hydrothermal Ore Deposits.* Wiley-Interscience, New York.

Bechtel A., Pervaz M. & Puttmann W. 1998. Role of organic matter and sulphate-reducing bacteria for metal sulphide precipitation in the Bahloul Formation at the Bou Grine Zn/Pb deposit (Tunisia). *Chemical Geology* **144**, 1–21.

Bechtel A., Shieh Y. N., Pervaz M. & Puttmann W. 1996. Biodegradation of hydrocarbons and biogeochemical sulfur cycling in the salt dome environment—inferences from sulfur isotope and organic geochemical investigations of the Bahloul Formation at the Bou Grine Zn/Pb ore deposit, Tunisia. *Geochimica et Cosmochimica Acta* **60**, 2833–2855.

Blum N. & Puchelt H. 1991. Sedimentary-hosted polymetallic massive sulphide deposits of the Kebrit and Shaban Deeps, Red Sea. *Mineralium Deposita* **26**, 217–227.

Bregant D., Catalano G., Civitarese G. & Luchetta A. 1990. Some chemical characteristics of the brines in Bannock and Tyro Basins: salinity, sulphur compounds, Ca , F, pH, A_t, PO_4, SiO_2, NH_3. *Marine Chemistry* **31**, 35–62.

Brown A. C. 1993. Sediment-hosted stratiform copper deposits. *In:* Sheahan P. & Cherry M. E. eds. *Ore Deposit Models Volume II*, Vol. 6, pp. 99–115. Geological Association of Canada Reprint Series.

Camerlenghi A. 1990. Anoxic basins of the eastern Mediterranean: geological framework. *Marine Chemistry* **31**, 1–19.

Carpenter A. B., Trout M. L. & Pickett E. E. 1974. Preliminary report on the origin and chemical evolution of oil field brines in central Mississippi. *Economic Geology* **69**, 1191–1206.

Charef A. & Sheppard S. M. F. 1987. Pb–Zn mineralisation associated with diapirism: fluid inclusion and stable isotope (H, C, O) evidence for the origin and evolution of the fluids at Fedj-el-Adoum, Tunisia. *Chemical Geology* **61**, 113–134.

Charef A. & Sheppard S. M. F. 1991. The diapir related Bou Grine Pb–Zn deposit (Tunisia); evidence for role of hot sedimentary basin brines. *In:* Pagel M. & Leroy J. L. eds. *Source, Transport and Deposition of Metals*, pp. 269–272. Balkema, Rotterdam.

Chartrand F. M., Brown A. C. & Kirkham R. V. 1989. Diagenesis, sulphides, and metal zoning in the Redstone copper deposit, Northwest Territories. *In:* Boyle R. W., Brown A. C., Jefferson

C. W., Jowett E. C. & Kirkham R. V. eds. *Sediment-hosted Stratiform Copper Deposits*, pp. 189–206. Geological Association of Canada Special Paper **36**.

Damore F., Giusti D. & Abdallah A. 1998. Geothermics of the high-salinity geothermal field of Asal, Republic of Djibouti, Africa. *Geothermics* **27**, 197–210.

Degens E. T. & Ross D. A. 1969. *Hot Brines and Recent Heavy Metal Deposits in the Red Sea.* Springer Verlag, New York.

Demaison G. J. & Moore G. T. 1980. Anoxic environments and oil source bed genesis. *American Association of Petroleum Geologists Bulletin* **64**, 1179–1209.

Dupre B., Blanc G., Boulegue J. & Allegre C. J. 1988. Metal remobilization at a spreading centre studied using lead isotopes. *Nature* **333**, 165–167.

El Tabakh M., Schreiber B. C., Utha-Aroon C., Coshell L. & Warren J. K. 1998. Diagenetic origin of Basal Anhydrite in the Cretaceous Maha Sarakham Salt – Khorat Plateau, NE Thailand. *Sedimentology* **45**, 579–594.

Emery D. & Robinson A. 1993. *Inorganic Chemistry: Applications to Petroleum Geology*. Blackwell Scientific Publications, Oxford.

Erba E. 1991. Deep mid-water bacterial mats from anoxic basins of the eastern Mediterranean. *Marine Geology* **100**, 83–101.

Eugster H. P. 1985. Oil shales, evaporites and ore deposits. *Geochimica et Cosmochimica Acta* **49**, 619–635.

Eugster H. P. 1989. Geochemical environments of sediment-hosted Cu–Pb–Zn deposits. *In:* Boyle R. W., Brown A. C., Jefferson C. W., Jowett E. C. & Kirkham R. V. eds. *Sediment-hosted Stratiform Copper Deposits*, pp. 111–126. Geological Association of Canada Special Paper **36**.

Fallara F., Savard M. M. & Paradis S. 1998. A structural, petrographic, and geochemical study of the Jubilee Zn–Pb deposit, Nova Scotia, Canada and a new metallogenic model. *Economic Geology* **93**, 757–778.

Ferguson J., Etminan H. & Ghassemi F. 1992. Salinity of deep formation water in the Canning Basin, Western Australia. *BMR Journal of Australian Geology & Geophysics* **13**, 93–105.

Ferguson J., Etminan H. & Ghassemi F. 1993. Geochemistry of deep formation waters in the Canning Basin, Western Australia, and their relationship to Pb–Zn mineralisation. *Australian Journal of Earth Sciences* **40**, 471–483.

Flint S. S. 1989. Sediment-hosted stratabound copper deposits of the Central Andes. *In:* Boyle R. W., Brown A. C., Jefferson C. W., Jowett E. C. & Kirkham R. V. eds. *Sediment-hosted Stratiform Copper Deposits*, pp. 371–398. Geological Association of Canada Special Paper **36**.

Fontboté L. & Gorzawski H. 1990. Genesis of the Mississippi Valley-type Zn–Pb deposit of San Vicente, Central Peru: Geologic and isotopic (Sr, O, C, S, Pb) evidence. *Economic Geology* **85**, 1402–1437.

Gablina I. F. 1981. New data on the formation conditions of the Dzhezkazgan copper deposit. *International Geology Review* **23**, 1311–1313.

Gablina I. F. 1997. Formation conditions of large cupriferous sandstone and shale deposits. *Geology of Ore Deposits* **39**, 320–333.

Ghazban F., Schwarcz H. P. & Ford D. C. 1990. Carbon and sulfur isotope evidence for in situ reduction of sulfate, Nanisivik lead-zinc deposits, Northwest Territories, Baffin Island, Canada. *Economic Geology* **85**, 360–375.

Grotzinger J. P. 1995. Trends in Precambrian carbonate sediments and their implication for understanding evolution. *In:* Bengtson S. ed. *Early Life on Earth: Nobel Symposium No. 84*, pp. 245–258. Columbia University Press, New York.

Grotzinger J. P. & Knoll A. H. 1995. Anomalous carbonate precipitates—Is the Precambrian the key to the Permian. *Palaios* **10**, 578–596.

Hanor J. S. 1994. Origin of saline fluids in sedimentary basins. *In:* Parnell J. ed. *Geofluids; Origin, Migration and Evolution of Fluids in Sedimentary Basins*, pp. 151–174. Geological Society of London Special Publication **78**.

Hartmann M., Scholten J. C., Stoffers P. & Wehner K. F. 1998. Hydrographic structure of the brine-filled deeps in the Red Sea—New results from the Shaban, Kebrit, Atlantis II, and Discovery deeps. *Marine Geology* **144**, 311–330.

Hein F. J., Graves M. C. & Ruffman A. 1991. The Jubilee zinc–lead deposit, Nova Scotia: the role of synsedimentary faults. *In:* Sangster A. L. ed. *Mineral Deposit Studies in Nova Scotia*. Geological Survey of Canada Paper **90-8**.

Henneke E., Luther G. W., Delange G. J. & Hoefs J. 1997. Sulphur speciation in anoxic hypersaline sediments from the Eastern Mediterranean Sea. *Geochimica et Cosmochimica Acta* **61**, 307–321.

Hill C. 1995. Sulfur redox reactions: hydrocarbons, native sulfur, Mississippi Valley-type deposits, and sulfuric acid karst in the Delaware Basin, New Mexico and Texas. *Environmental Geology* **25**, 16–23.

Huber R., Kurr M., Jannasch H. W. & Stetter K. O. 1989. A novel group of methanogenic archaebacteria (*Methanopyrus*) growing at 110°C. *Nature* **342**, 833–834.

Huichi R., Renmin H. & Cox D. P. 1991. Copper deposition by fluid mixing in deformed strata adjacent to a salt diapir, Dongchuan area, Yunnan Province, China. *Economic Geology* **86**, 1539–1545.

Huyck H. L. O. & Chorey R. W. 1991. Stratigraphic and petrographic comparison of the Creta and Kupferschiefer copper shale deposits. *Mineralium Deposita* **26**, 132–142.

Jackson M. P. A., Vendeville B. C. & Shultz-Ela D. D. 1994. Structural dynamics of salt systems. *Annual Review of Earth and Planetary Sciences* **22**, 93–117.

Jowett E. C. 1992. Role of organics and methane in sulfide ore formation, exemplified by Kupferschiefer Cu–Ag deposits, Poland. *Chemical Geology* **99**, 51–63.

Jowett E. C., Rydzewski A. & Jowett R. J. 1987. The Kupferschiefer Cu–Ag ore deposits in Poland: a re-appraisal of the evidence of their origin and presentation of a new genetic model. *Canadian Journal of Earth Sciences* **24**, 2016–2037.

Jørgensen B. B., Isaksen M. F. & Jannasch H. W. 1992. Bacterial sulfate reduction above 100°C in deep-sea hydrothermal vent sediments. *Science* **258**, 1756–1757.

Kennicutt II M. C., Brooks J. M., Bidigare R. R., Fay R. R., Wade T. L. & McDonald T. J. 1985. Vent-type taxa in a hydrocarbon seep region on the Louisiana slope. *Nature* **317**, 351–353.

Kesler S. E., Jones H. D., Furman F. C., Sassen R., Anderson W. H. & Kyle J. R. 1994. Role of crude oil in the genesis of Mississippi Valley-Type deposits; evidence from the Cincinnati Arch. *Geology* **22**, 609–612.

Kharaka Y. K., Carothers W. W., Law L. M., Lamonthe P. J. & Fries T. L. 1987. Geochemistry of metal-rich brines from the central Mississippi Salt Dome Basin, USA. *Applied Geochemistry* **2**, 543–562.

Kirkham R. V. 1989. Distribution, settings, and genesis of sediment-hosted stratiform copper deposits. *In:* Boyle R. W., Brown A. C., Jefferson C. W., Jowett E. C. & Kirkham R. V. eds. *Sediment-hosted Stratiform Copper Deposits*, pp. 3–38. Geological Association of Canada Special Paper **36**.

Kontak D. J., Farrar E. & McBride S. L. 1994. Ar^{40}–Ar^{39} dating of fluid migration in a Mississippi-Valley type deposit—The Gays River deposit, Nova Scotia, Canada. *Economic Geology* **89**, 1501–1517.

Kontak D. J. & Jackson S. 1995. Laser-ablation ICP-MS microanalysis of calcite cement from a Mississippi-Valley type Zn–Pb deposit, Nova Scotia—Dramatic variability in REE content on macro- and micro-scales. *Canadian Mineralogist* **33**, 445–467.

Krouse H. R., Vian C. A., Eliuk L. S., Ueda A. & Halas S. 1988. Chemical and isotopic evidence of thermochemical sulphate reduction by light hydrocarbon gases in deep carbonate reservoirs. *Nature* **333**, 415–419.

Kyle J. R. 1991. Evaporites, evaporitic processes and mineral resources. *In:* Melvin J. L. ed. *Evaporites, Petroleum and Mineral Resources*, pp. 477–533. Developments in Sedimentology **50.** Elsevier, Amsterdam.

Kyle J. R. & Posey H. H. 1991. Halokinesis, cap rock development and salt dome mineral resources. *In:* Melvin J. L. ed. *Evaporites, Petroleum and Mineral Resources*, pp. 413–474. Developments in Sedimentology **50.** Elsevier, Amsterdam.

Kyle J. R. & Price P. E. 1986. Metallic sulphide mineralisation in salt-dome cap rocks, Gulf Coast, U.S.A. *Transactions of the Institution of Mining and Metallurgy Section B: Applied Earth Sciences* **95**, B6–B16.

Land L. S. 1995a. Na–Ca–Cl saline formation waters, Frio Formation (Oligocene), south Texas, USA: products of diagenesis. *Geochimica et Cosmochimica Acta* **59**, 2163–2174.

Land L. S. 1995b. The role of saline formation water in crustal cycling. *Aquatic Geochemistry* **1**, 137–145.

Land L. S. & Prezbindowski D. R. 1981. The origin and evolution of

saline formation water, Lower Cretaceous carbonates, South-central Texas, USA. *Journal of Hydrology* **54**, 51–74.

Large D. J. & Gize A. P. 1996. Pristane/phytane ratios in the mineralized Kupferschiefer of the Fore-Sudetic Monocline, southwest Poland. *Ore Geology Reviews* **11**, 89–103.

Lavoie D., Sangster D. F., Savard M. M. & Fallara F. 1998. Breccias in the lower part of the Mississippian Windsor Group and their relation to Pb–Zn mineralisation: a summary. *Economic Geology* **93**, 734–735.

Lebedev L. M. 1972. Minerals of contemporary hydrotherms of Cheleken. *Geochemistry International* **9**, 485–504.

Light M. P. R. & Posey H. H. 1992. Diagenesis and its relation to mineralisation and hydrocarbon reservoir development; Gulf Coast and North Sea Basins. *In:* Wolf K. H. & Chilingarian G. V. eds. *Diagenesis III*, pp. 511–541. Developments in Sedimentology **47**. Elsevier, Amsterdam.

Logan G. A., Hayes J. M., Hieshima G. B. & Summons R. E. 1995. Terminal Proterozoic reorganisation of biogeochemical cycles. *Nature* **376**, 53–56.

Lynch G., Keller J. V. A. & Giles P. S. 1998. Influence of the Ainslie Detachment on the stratigraphy of the Maritimes Basin and mineralisation in the Windsor Group of Northern Nova Scotia, Canada. *Economic Geology* **93**, 703–718.

Lynch G. & Keller J. V. A. 1998. Association between detachment faulting and salt diapirs in the Devonian–Carboniferous Maritimes Basin, Atlantic Canada. *Bulletin of Canadian Petroleum Geology* **46**, 189–209.

Machel H. G., Krouse H. R. & Sassen R. 1995. Products and distinguishing criteria of bacterial and thermochemical sulfate reduction. *Applied Geochemistry* **10**, 373–389.

Martens C. S., Chanton J. P. & Paull C. K. 1991. Biogenic methane from abyssal brine seeps at the base of the Florida Escarpment. *Geology* **19**, 851–854.

Monnin C. & Ramboz C. 1996. The anhydrite saturation index of the ponded brines and sediment pore waters of the Red Sea deeps. *Chemical Geology* **127**, 141–159.

Montacer M., Disnar J. R., Orgeval J. J. & Trichet J. 1988. Relationship between Zn–Pb ore and oil accumulation processes; example of the Bou Grine Deposit (Tunisia). *Organic Geochemistry* **13**, 423–431.

Moritz R., Fontboté L., Spangenberg J., Rosas S., Sharp Z. & Fontignie D. 1996. Sr, C and O isotope systematics in the Pucara Basin, central Peru: comparison between Mississippi Valley-type deposits and barren areas. *Mineralium Deposita* **31**, 147–162.

Morrison S. J. & Parry W. T. 1986. Formation of carbonate–sulfate veins associated with copper ore deposits from saline basin brines, Lisbon Valley, Utah: fluid inclusion and isotopic evidence (USA). *Economic Geology* **81**, 1853–1866.

Noth S. 1997. High H_2S contents and other effects of thermochemical sulphate reduction in deeply buried carbonate reservoirs. *Geologische Rundschau* **86**, 275–287.

Orgeval J. J. 1991. A new type of Zn–Pb concentration related to salt dome activity: example of the Bou Grine deposit (Tunisian Atlas). *In:* Pagel M. & Leroy J. L. eds. *Source, Transport and Deposition of Metals*, pp. 269–272. Balkema, Amsterdam.

Orgeval J. J. 1994. Peridiapiric metal concentration: example of the Bou Grine deposit (Tunisian Atlas). *In:* Fontboté L. & Boni M. eds. *Sediment-hosted Zn–Pb Ores*, pp. 354–388. Society of Geology Applied to Mineral Deposits, Special Publication **10**.

Oszczepalski S. 1989. Kupferschiefer in southwestern Poland: sedimentary environments, metal zoning, and ore controls. *In:* Boyle R. W., Brown A. C., Jefferson C. W., Jowett E. C. & Kirkham R. V. eds. *Sediment-hosted Stratiform Copper Deposits*, pp. 571–600. Geological Association of Canada Special Paper **36**.

Oszczepalski S. 1994. Oxidative alteration of the Kupferschiefer in Poland: oxide–sulphide parageneses and implications for ore-forming models. *Kwartalnik Geologiczny* **38**, 651–671.

Peng Q. M. & Palmer M. R. 1995. The Palaeoproterozoic boron deposits in eastern Liaoning, China: a metamorphosed evaporite. *Precambrian Research* **72**, 185–197.

Pottorf R. J. & Barnes H. L. 1983. Mineralogy, geochemistry, and ore genesis of hydrothermal sediments from the Atlantis II Deep, Red Sea. *Economic Geology Monographs* **5**, 198–223.

Price P. E., Kyle J. R. & Wessel G. R. 1983. Salt dome related Zn–Pb deposits. *In:* Kisvarsanyi G. ed. *Proceedings, International Conference on Mississippi Valley Type Lead-Zinc Deposits*, pp. 558–571. University of Missouri, Rolla.

Raiswell R. & Al-Biatty H. J. 1992. Depositional and diagenetic C–S–Fe signatures and the potential of shales to generate metal-rich fluids. *In:* Schidlowski M. ed. *Early Organic Evolution: Implications for Mineral and Energy Resources*, pp. 415–425. Springer-Verlag, Berlin.

Ramboz C. & Danis M. 1990. Superheating in the Red Sea? The heat-mass balance of the Atlantis II Deep revisited. *Earth and Planetary Science Letters* **97**, 190–210.

Ravenhurst C. E., Reynolds P. H. & Zentilli M. 1987. A model for the evolution of hot (>200 degrees C) overpressured brines under an evaporite seal; the Fundy/Magdalen Carboniferous basin of Atlantic Canada and its associated Pb–Zn–Ba deposits. *Atlantic Geoscience Society* **23**, 105.

Riciputi L. R., Cole D. R. & Machel H. G. 1996. Sulfide formation in reservoir carbonates of the Devonian Nisku Formation, Alberta, Canada—an ion microprobe study. *Geochimica et Cosmochimica Acta* **60**, 325–336.

Roberts H. H., Aharon P., Carney R., Larkin J. & Sassen R. 1990. Sea floor responses to hydrocarbon seeps, Louisiana continental slope. *Geo-marine Letters* **10**, 232–243.

Rouvier H., Perthuisot V. & Mansouri A. 1985. Pb–Zn deposits and salt-bearing diapirs in southern Europe and North Africa. *Economic Geology* **80**, 666–687.

Rowan M. G. 1995. Structural styles and evolution of allochthonous salt, central Louisiana outer shelf and upper slope. *In:* Jackson M. P. A. , Roberts D. G. & Snelson S. eds. *Salt Tectonics; a Global Perspective*, pp. 199–228. American Association of Petroleum Geologists Memoir **65**.

Ruelle J. C. L. 1982. Depositional environments and genesis of stratiform copper deposits of the Redstone copper belt, Mackenzie Mountains, NWT. *In:* Hutchison R. W., Spence C. D. & Franklin J. M. eds. *Precambrian Sulphide Deposits*, pp. 701–737. Geological Association of Canada Special Paper **25**.

Sangster D. F., Savard M. M. & Kontak D. J. 1998. A genetic model for the mineralisation of Lower Windsor (Visean) carbonate rocks of Nova Scotia, Canada. *Economic Geology* **93**, 932–952.

Savard M. M. 1996. Pre-ore burial dolomitization adjacent to the carbonate-hosted Gays River Zn–Pb deposit, Nova Scotia. *Canadian Journal of Earth Sciences* **33**, 302–315.

Sawlowicz Z. 1992. Primary sulphide mineralisation in Cu–Fe–S zones of Kupferschiefer, Fore-Sudetic monocline, Poland. *Transactions of the Institution of Mining and Metallurgy Section B: Applied Earth Sciences* **101**, B1–B8.

Shanks III W. C. 1983. Economic and exploration significance of Red Sea metalliferous brine deposits. *In:* Shank III W. C. ed. *Cameron Volume on Unconventional Mineral Deposits*, pp. 157–171. American Institute of Mining, Metallurgical and Petroleum Engineers Monograph.

Shanks III W. C. & Bischoff J. L. 1980. Geochemistry, sulfur isotope composition, and accumulation rates of Red Sea geothermal deposits. *Economic Geology* **75**, 445–459.

Sheu D. D. 1987. Sulfur and organic carbon contents in sediment cores from the Tyro and Orca basins. *Marine Geology* **75**, 157–164.

Spangenberg J., Fontboté L., Sharp Z. D. & Hunziker J. 1996. Carbon and oxygen isotope study of hydrothermal carbonates in the zinc–lead deposits of the San Vicente district, Central Peru—Quantitative modelling of mixing processes and CO_2 degassing. *Chemical Geology* **133**, 289–315.

Susura B. B., Glybovsky V. O. & Kislitsin A. V. 1986. Red-colored terrigenous sediments; specific copper-forming systems. *In:* Friedrich G. H., Genkin A. D., Naldrett A. J., Ridge J. D., Sillitoe R. H. & Vokes F. M. eds. *Geology and Metallogeny of Copper Deposits*, pp. 504–512. Springer-Verlag, Berlin.

Sverjensky D. A. 1986. Genesis of Mississippi Valley-type lead-zinc deposits. *Annual Review of Earth and Planetary Sciences* **14**, 177–199.

Sverjensky D. A. 1989. Chemical evolution of basinal brines that formed sediment-hosted Cu-Pb-Zn deposits. *In:* Boyle R. W., Brown A. C., Jefferson C. W., Jowett E. C. & Kirkham R. V. eds. *Sediment-hosted Stratiform Copper Deposits*, pp. 127–134. Geological Association of Canada Special Paper **36**.

Thrasher J., Fleet A. J., Hay S. J., Hovland M. & Düppenbecker S. 1996. Understanding geology as the key to using seepage in exploration:

the spectrum of seepage styles. *In:* Schumacher D. & Abrams M. A. eds. *Hydrocarbon Migration and its Near-Surface Expression*, pp. 223–241. American Association of Petroleum Geologists Memoir **66**.

Tompkins L. A., Rayner M. J., Groves D. I. & Roche M. T. 1994. Evaporites; in situ sulfur source for rhythmically banded ore in the Cadjebut Mississippi valley-type Zn–Pb deposit, Western Australia. *Economic Geology* **89**, 467–492.

Trefry J. H., Presley B. J., Keeney-Kennicutt W. L. & Trocine R. P. 1984. Distribution and chemistry of manganese, iron, and suspended particulates in Orca Basin. *Geo-marine Letters* **4**, 125–130.

Trudinger P. A., Chambers L. A. & Smith J. W. 1985. Low-temperature sulphate reduction; biological versus abiological. *Canadian Journal of Earth Sciences* **22**, 1910–1918.

Vaughan D. J., Sweeney M., Friedrich G., Diedel R. & Haranczyk C. 1989. The Kupferschiefer: an overview with an appraisal of the different types of mineralisation. *Economic Geology* **84**, 1003–1027.

Wang A. J., Peng Q. M. & Palmer M. R. 1998. Salt dome-controlled sulphide precipitation of Palaeoproterozoic Fe–Cu sulphide deposits, eastern Liaoning, Northeastern China. *Economic Geology* **93**, 1–14.

Warren J. K. 1996. Evaporites, brines and base metals: what is an evaporite? Defining the rock matrix. *Australian Journal of Earth Sciences* **43**, 115–132.

Warren J. K. 1997. Evaporites, brines and base metals: brines, flow and 'the evaporite that was'. *Australian Journal of Earth Sciences* **44**, 149–183.

Warren J. K. 1999. *Evaporites: Their Evolution and Economics*. Blackwell Science, Oxford.

Warren J. K., George S. C., Hamilton P. J. & Tingate P. 1998. Proterozoic source rocks—Sedimentology and organic characteristics of the Velkerri Formation, Northern Territory, Australia. *American Association of Petroleum Geologists Bulletin* **82**, 442–463.

Warren J. K. & Kempton R. H. 1997. Evaporite sedimentology and the origin of evaporite-associated Mississippi Valley-type sulfides in the Cadjebut Mine Area, Lennard Shelf, Canning Basin, Western Australia. *In:* Moñtanez I. P., Gregg J. M. & Shelton K. L. eds. *Basinwide Diagenetic Patterns: Integrated Petrologic, Geochemical, and Hydrologic Considerations*, pp. 183–205. Society of Economic Paleontologists and Mineralogists Special Publication **57**.

Werner M. L., Feldman M. D. & Knauth L. P. 1988. Petrography and geochemistry of water–rock interactions in Richton Dome cap rock (southeastern Mississippi, U.S.A.). *Chemical Geology* **74**, 113–135.

Williams D. F. & Lerche I. 1987. Salt domes, organic-rich source beds and reservoirs in intraslope basins of the Gulf Coast region. *In:* Lerche I. & O'Brien J. J. eds. *Dynamical Geology of Salt and Related Structures*, pp. 751–830. Academic Press, New York.

Wodzicki A. & Piestrzynski A. 1994. An ore genetic model for the Lubin–Sieroszowice mining district. *Mineralium Deposita* **29**, 30–43.

Worden R. H. & Smalley P. C. 1996. H_2S-producing reactions in deep carbonate gas reservoirs—Khuff Formation, Abu Dhabi. *Chemical Geology* **133**, 157–171.

Worden R. H., Smalley P. C. & Fallick A. E. 1997. Sulfur cycle in buried evaporites. *Geology* **25**, 643–646.

Worden R. H., Smalley P. C. & Oxtoby N. H. 1995. Gas souring by thermochemical sulfate reduction at 140° C. *American Association of Petroleum Geologists Bulletin* **79**, 854–863.

Worden R. H., Smalley P. C. & Oxtoby N. H. 1996. The effects of thermochemical sulphate reduction upon formation water salinity and oxygen isotopes in carbonate gas reservoirs. *Geochimica et Cosmochimica Acta* **60**, 3925–3931.

Wu M. & Xiji L. 1981. Two types of diapiric structure of the Kunyang Group, Yunnan (in Chinese). *Acta Geologica Sinica* **55**, 105–117.

Zierenberg R. A. & Shanks III W. C. 1983. Mineralogy and geochemistry of epigenetic features in metalliferous sediment, Atlantis II Deep, Red Sea. *Economic Geology* **78**, 57–72.

Received 9 August 1999; accepted 14 January 2000